Title

Swelling-activated chloride channels in multidrug-sensitive and -resistant cells.

Journal

The Journal of General Physiology, 104(6)

ISSN

0022-1295

Authors

Ehring, GR
Osipchuk, YV
Cahalan, MD

Publication Date

1994-12-01

DOI

10.1085/jgp.104.6.1129

Swelling-activated Chloride Channels in Multidrug-sensitive and -resistant Cells

GEORGE R. EHRING, YURI V. OSIPCHUK, and MICHAEL D. CAHALAN

From the Department of Physiology and Biophysics, University of California at Irvine, Irvine, California 92717

ABSTRACT Resistance to chemotherapeutic agents in neoplastic cells is often mediated by expression of P-glycoprotein, which functions as a drug-efflux pump for a broad range of substrates. We have used a combination of patch clamp and video-imaging techniques to examine the expression and drug-efflux function of P-glycoprotein and to determine the possible correlation with swelling-activated chloride channels in drug-sensitive and -resistant cell lines. Two pairs of cell lines were used in these experiments: (*a*) control NIH-3T3 cells and a corresponding *MDR1*-transfectant; and (*b*) control 8226 myeloma cells and a derivative cell line selected for resistance to chemotherapeutic agents. Control cells lacked detectable P-glycoprotein expression based on Western blotting, immunofluorescence staining with a specific monoclonal antibody, and a functional assay of rhodamine-123 (R123) efflux. Resistant cells expressed P-glycoprotein at high levels and rapidly exported R123. During whole-cell recording using either hyperosmotic pipette solution or hypoosmotic Ringer solution, cell swelling was accompanied by Cl^- channel opening in all four cell lines. The rates of induction, biophysical properties and magnitudes of Cl^- conductance (g_{Cl}) were indistinguishable between control and corresponding multidrug-resistant cells: g_{Cl} reached 0.96 ± 0.31 (n = 14) and 0.83 ± 0.31 nS/pF (mean ± SD; n = 31) in NIH-3T3 and NIH-3T3/MDR cells, respectively; and 0.31 ± 0.20 (n = 9) and 0.37 ± 0.22 nS/pF (n = 7) in 8226 and 8226/Dox_{40} cells, respectively. g_{Cl} exhibited moderate outward rectification in symmetrical Cl^- solutions, with a rectification ratio of 1.4 at ± 50 mV. Cl^- channels slowly closed during strong depolarization beyond +60 mV. Using video-imaging techniques with SPQ as a fluorescent probe, we monitored Cl^--channel opening in intact drug-sensitive and -resistant cells. g_{Cl}, measured either with whole-cell recording or SPQ imaging, was blocked by DIDS (voltage-dependent K_d < 50 μM at +40 mV), NPPB (K_d ~ 30 μM), and tamoxifen (complete and irreversible block ~10 μM). None of these blockers inhibited R123 efflux. NPPB accelerated R123 efflux, an effect that was mimicked by CCCP, a mitochondrial uncoupler. In contrast, verapamil selectively blocked R123 efflux (K_d = 0.3 to 0.5 μM); 10 μM left g_{Cl} unaltered. Induction of g_{Cl} was not affected by vincristine or doxorubicin in the pipette solution. Moreover, the rate of R123 efflux did not change during cell swelling. We conclude that P-glycoprotein and swelling-activated chloride channels function independently and are separable by expression and by pharmacological sensitivities.

Address correspondence to Michael D. Cahalan, Department of Physiology and Biophysics, University of California at Irvine, Irvine, CA 92717.

J. GEN. PHYSIOL. © The Rockefeller University Press · 0022-1295/94/12/1129/33 $2.00
Volume 104 December 1994 1129–1161

INTRODUCTION

When exposed to changes in extracellular osmolarity, many mammalian cells regulate their volume by coupling water flux to osmolyte transport across the cell membrane. K^+ and Cl^- currents contribute a large fraction of the total osmolyte flux (Hoffmann and Simonsen, 1989). In particular, swelling-activated Cl^- channels may be important in triggering and maintaining the ionic flux required for volume regulation (Cahalan and Lewis, 1988, 1994). Although only cells within the kidney or digestive tract are likely to experience large changes in osmolarity, swelling-activated Cl^- channels are found in many epithelia and other tissues. Thus, swelling-activated Cl^- channels may serve alternative functions such as epithelial fluid transport or volume regulation during cell division or motility.

The molecular characterization of Cl^- channels provides significant insight into their structure and function. Unlike the families of homologous proteins that form K^+, Ca^{2+}, and Na^+ channels, there is a wide diversity of molecules that form Cl^- channels (for review, see Frizzell and Cliff, 1992). Without highly conserved structural motifs to distinguish potential channel-forming molecules, and because there are no specific toxins or potent pharmacological agents to aid in their identification, each candidate Cl^- channel must be carefully evaluated for function and expression. Such a detailed analysis, including biophysical, biochemical, and molecular biological characterization, has been performed on the cystic fibrosis transmembrane conductance regulator (CFTR), indicating that the CFTR can form one type of Cl^- channel (reviewed by Welsh, Anderson, Rich, Berger, Denning, Ostedgaard, Sheppard, Cheng, Gregory, and Smith, 1992).

The CFTR belongs to the ABC (ATP-binding cassette) superfamily. A second member of this family, P-glycoprotein—the *MDR1* gene product, is an ATP-dependent transporter responsible for multidrug resistance to a broad spectrum of chemotherapeutic agents (Higgins, 1992; Gottesman and Pastan, 1993). P-glycoprotein is endogenously expressed in several epithelial tissues, which may also express swelling-activated Cl^- channels (Hitchins, Harman, Davey, and Bell, 1988; Arceci, Baas, Raponi, Horwitz, Housman, and Croop, 1990; van Kalken, van der Valk, Hadisaputro, Pieters, Broxterman, Kuiper, Scheffer, Veerman, Meyer, and Scheper, 1991; van Kalken, Giaccone, van der Valk, Kuiper, Hadisaputro, Bosma, Scheper, Meijer, and Pinedo, 1992; Toth, Vaughan, Slocum, Arredondo, Takita, Baker, and Rustum, 1994). Valverde and co-workers (1992), based on evidence that transfection of the *MDR1* gene into NIH-3T3 fibroblasts or into S1 lung carcinoma cells resulted in the expression of both P-glycoprotein and swelling-activated Cl^- channels, suggested that P-glycoprotein has two distinct functions: an ATP hydrolysis-dependent drug-transport pump or a swelling-activated Cl^- channel that requires ATP binding, but not hydrolysis. In their model (Gill, Hyde, Higgins, Valverde, Mintenig, and Sepulveda, 1992), cell swelling traps P-glycoprotein in its Cl^- channel conformation, thus making it unavailable to pump drugs. Conversely, drug binding and transport traps P-glycoprotein in its pump conformation, preventing the induction of its Cl^- conductance (g_{Cl}) by subsequent cell swelling.

Recently, however, several studies have indicated a lack of correlation between P-glycoprotein expression and g_{Cl}. T_{84} colonic adenocarcinoma cells, which express

P-glycoprotein, showed similar rates of transepithelial secretion of vinblastine, an antineoplastic agent, whether or not they exhibited g_{Cl} (McEwan, Hunter, Hirst, and Simmons, 1992). Rasola, Galietta, Gruenert, and Romeo, (1994), using epithelial cell lines selected for drug resistance, found no correlation between P-glycoprotein expression and g_{Cl}. In addition, hypoosmotic stress did not affect the accumulation of rhodamine-123 (R123), a substrate for P-glycoprotein transport, in mouse lymphoma cells transduced with the *MDR1* gene (Weaver, Szabo, Pine, Gottesman, Goldenberg, and Aszalos, 1993). Altenberg, Vanoye, Han, Deitmer, and Reuss (1994*b*) found that multidrug-resistant Chinese hamster fibroblasts, which express high levels of P-glycoprotein, did not express swelling-activated Cl^- channels. However, they also observed g_{Cl} in human breast cancer cells (BC19/3) rendered multidrug-resistant by transfection with the human *MDR1* gene; such currents were not observed in the parental drug-sensitive cell line (MCF-7). Interestingly, neither BC19/3 nor MCF-7 cells volume-regulate or permit measurable amounts of Cl^- efflux under hypoosmotic stress (Altenberg, Deitmer, Glass, and Reuss, 1994*a*).

We have further tested the hypothesis of Valverde et al. (1992) that swelling-activated chloride currents are associated with increased expression of human P-glycoprotein after (*a*) transfection with the *MDR1* gene or (*b*) selection for multidrug resistance. Four cell lines were evaluated for both chloride conductance and P-glycoprotein-mediated substrate efflux: (*a*) the drug-sensitive 8226 human myeloma cell line; (*b*) its drug-resistant derivative line, 8226/Dox_{40} (Dalton, Grogan, Rybski, Scheper, Richter, Kailey, Broxterman, Pinedo, and Salmon, 1989); (*c*) control NIH-3T3 mouse fibroblasts; and (*d*) NIH-3T3/MDR cells permanently transfected with the human *MDR1* gene (Ueda, Cardarelli, Gottesman, and Pastan, 1987; Kioka, Tsubota, Kakehi, Komano, Gottesman, Pastan, and Ueda, 1989; Bruggemann, Currier, Gottesman, and Pastan, 1992). Initially, we measured g_{Cl} induced by osmotically driven cell swelling, using conventional whole-cell recording. In addition, we used video-imaging techniques to monitor both P-glycoprotein substrate efflux and swelling-activated chloride conductance in intact cells. We show that P-glycoprotein–mediated drug efflux and swelling-activated chloride conductance are separable functions, both pharmacologically and by mode of activation. Our results indicate that there is no correlation between P-glycoprotein and Cl^- channel expression. These results have been presented in preliminary form (Ehring, Osipchuk, and Cahalan, 1994; Osipchuk, Ehring, and Cahalan, 1994).

MATERIALS AND METHODS

Cells

The drug-sensitive 8226 myeloma cell line and the drug-resistant 8226/Dox_{40} cell line were obtained from Dr. William Dalton (Arizona Cancer Center, University of Arizona, Tuscon, AZ). Both cell lines were cultured in suspension at 37°C in 5% CO_2 and maintained in RPMI 1640 medium containing 25 mM *N*-hydroxyethylpiperazine-*N'*-2-ethanesulfonic acid (HEPES) supplemented with 10% fetal bovine serum (FBS), 1% penicillin streptomycin (P-S) and 1% L-glutamine. 8226/Dox_{40} cells were also treated with 4×10^{-7} M doxorubicin every two weeks. These cells were fed twice weekly and split weekly. For patch clamp experiments, the cells were plated on glass coverslips which had been pretreated with 1 mg/ml poly-L-lysine.

NIH-3T3 fibroblasts and NIH-3T3 fibroblasts transfected with the pHa MDR (Gly185) clone

of *MDR1* were obtained from Dr. Michael Gottesmann (National Cancer Institute, National Institutes of Health, Bethesda, MD). Both lines were cultured as monolayers at 37°C in 5% CO_2 using DMEM containing 25 mM HEPES and supplemented with 4.5 g glucose per liter, 10% FBS, 1% P-S and 1% L-glutamine. The medium for the *MDR1* transfectant was supplemented with 60 ng/ml colchicine. We confirmed the increased expression of P-glycoprotein in the drug-resistant lines by immunoblotting. Membrane preparations from all four cell lines were run on SDS-PAGE gels, immunoblotted, and stained by an antibody (C219) to a cytoplasmic carboxy-terminal epitope of P-glycoprotein (Georges, Bradley, Gariepy, and Ling, 1990).

Solutions and Reagents

For most of the patch-clamp experiments, the cells were bathed in mammalian Ringer containing (in millimolar): 160 NaCl, 4.5 KCl, 2 $CaCl_2$, 1 $MgCl_2$, 0.1 BaCl and 10 HEPES, adjusted to pH 7.4 with NaOH and having an osmolarity of 310 mosm. Hypoosmotic Ringer (67% Ringer) was prepared by diluting mammalian Ringer with deionized (MilliQ) H_2O (Millipore Corp., Milford, MA). Pipette (internal) solutions contained 160 Cs aspartate, 2 $MgCl_2$, 5 HEPES, and 10 ethylene glycol-bis (β-aminoethylether) *N,N,N′,N′*-tetraacetic acid (EGTA), pH adjusted to 7.2 with KOH; 310 mosm. Hyperosmotic internal solution was prepared by adding 100 mM sucrose to the pipette solution. In some experiments, the cells were patch clamped with a pipette solution containing (in millimolar): 140 *N*-methyl-D-glucamine chloride (NMG-Cl), 1.2 $MgCl_2$, 1 mM EGTA and 10 mM HEPES with 2 mM NaATP adjusted to pH 7.4 (310 mosm). In these experiments, the cells were initially bathed in isoosmotic NMG-Cl Ringer containing (in millimolar): 140 NMG-Cl, 1.3 mM $CaCl_2$, 0.5 $MgCl_2$ and 10 mM HEPES (pH 7.4, 310 mosm). Hypoosmotic (70%) Ringer was made by reducing NMGCl to 105 mM. Osmolarity was measured with a vapor pressure osmometer (Wescor Inc., Logan, UT). Bath solutions were exchanged by perfusing the chamber (~250 μl vol) with 2–5 ml of the test solution. Exchange was complete in <30 s. Chloride was replaced by either iodide or nitrate for video-imaging measurements of chloride conductance. Iodide solution: 135 NaI, 2.4 K_2HPO_4, 0.6 KH_2PO_4, 1 $MgSO_4$, 1 $CaSO_4$, 10 HEPES (pH 7.4, adjusted with NaOH). Nitrate solution: 135 $NaNO_3$, 2.4 K_2HPO_4, 0.6 KH_2PO_4, 1 $MgSO_4$, 1 $CaSO_4$, 10 HEPES (pH 7.4, adjusted with NaOH). Normal osmolarity was adjusted to 310 mosm. Hypoosmotic solutions (50–90% of normal osmolarity) were prepared by diluting solutions with MilliQ water.

Most salts and reagents (reagent grade or better) were obtained from Sigma Chemical Co. (St. Louis, MO). Doxorubicin, vincristine and verapamil were obtained from Sigma Chemical Co. and 5-nitro-2-(3-phenylpropylamino) benzoic acid (NPPB) from Biomol Research Laboratories, Inc. (Philadelphia, PA). Rhodamine-123 (R123), 6-methoxy-*N*-(sulfopropyl)quinolinium (SPQ) and 4,4′-diisothiocyanatostilbene-2,2′-disulfonic acid (DIDS) were obtained from Molecular Probes, Inc. (Eugene, OR). All drugs were dissolved in DMSO at a stock concentration at least 1,000 times greater than the final bath concentration.

The 4E3 monoclonal IgG antibody specific to an extracellular epitope on P-glycoprotein, and C219 monoclonal antibody to an intracellular epitope on P-glycoprotein were obtained from Signet Laboratories (Dedham, MA). FITC-conjugated and Texas red-conjugated goat $F(ab')_2$ anti–mouse IgG were obtained from Caltag Laboratories (South San Francisco, CA).

Flow Cytometry

Aliquots of ~1 × 10^6 cells were taken directly from 8226 myeloma or 8226/Dox_{40} suspension cultures, or after trypsinization of NIH-3T3 control and NIH-3T3/MDR cell-adherent cultures, and resuspended in 100 μl phosphate buffered saline supplemented with 0.1% fetal calf serum (PBS/FCS). Primary antibodies (0.5 μg), either isotypic control IgG or monoclonal 4E3, were added to the cell suspension, vortexed for 3–5 s and incubated for 25 min at room

temperature. Unbound primary antibody was removed by dilution into 1 ml PBS/FCS followed by centrifugation at 300 *g* for 5 min. The wash procedure was repeated twice and the cells resuspended in 100 μl PBS/FCS containing ~0.5 μg FITC-conjugated goat $F(ab')_2$ anti–mouse IgG. The cells were vortexed for 3–5 s and incubated in the dark for 25 min at room temperature. Unbound $F(ab')_2$ fragments were removed as described for the primary antibody. Cell fluorescence was measured on a FACScan® flow cytometer (Becton Dickinson, Mountain View, CA). FITC fluorescence was excited by 150 mW of 488-nm light from an argon laser, and the emitted light was passed to a photomultiplier tube through a 530 ± 15 nM band pass filter (FL-1). Frequency histograms of the logarithm of the fluorescence were calculated for ~5,000 cells from each cell line using LYSIS II software (Becton Dickinson).

Confocal Microscopy

To measure protein expression and functional drug transport, cells were simultaneously labeled for P-glycoprotein expression with 4E3 antibody and incubated with R123. In drug-sensitive cells, R123 diffuses across the cell membrane, enters the cytoplasm and gets trapped within the mitochondria because of the mitochondrial membrane potential. In drug-resistant cells, the P-glycoprotein pump keeps the cytoplasmic concentration of R123 low and prevents accumulation within mitochondria. For these experiments, cells were adhered to glass coverslips in normal culture medium overnight in the incubator. The following day, cells were washed with mammalian Ringer then incubated at room temperature for 1.5 h with 5 μM R123 in Ringer ± 10 μM verapamil. During the first half hour of incubation, the Ringer solution also contained 4E3 antibody. The cells were then washed two times with fresh Ringer containing 5 μM R123. During the last half hour of R123 incubation, the cells were labeled with Texas red-conjugated goat $F(ab')_2$ anti–mouse IgG. Treated cells were placed on the confocal microscope and washed twice with normal medium.

The confocal microscope system consisted of a Nikon Labophot upright microscope with a Bio-Rad MRC-600 confocal laser scanner equipped with a krypton/argon laser (Bio-Rad Co., Hercules, CA). The light path included selectable excitation filters at 488 or 568 nm, a double dichroic mirror with near total reflectance for wavelengths of 488 and 568 nM and high transmission of wavelengths between 500 and 550 nm or wavelengths >600 nm. Texas red emission was measured, after excitation at 568 nm, as the intensity of light transmitted through a second dichroic mirror (>560 nm) and through a 585-nm long-pass emission filter to a photomultiplier tube (PMT1). R123 emission was measured, following excitation at 488 nm, as the light reflected by the second dichroic mirror (<560 nm) and passing through a 522-nm band pass filter to a second photomultiplier tube (PMT2). Because of the wide band widths for both emission and excitation of R123, the fluorescence for the double-labeled cells was measured in two sequential images. The first image was taken using 488-nm excitation to collect R123 (green) fluorescence, and the second used 568-nm excitation to collect Texas red (red) fluorescence. This procedure eliminated spectral overlap between the two dyes. Transmitted light images were taken by replacing the filter cube for PMT2 with a fiber optic which collected the light passing directly through the specimen.

Patch Clamp Recording

Experiments were carried out using standard whole-cell patch clamp recording techniques (Lewis, Ross, and Cahalan, 1993). All experiments were done at room temperature (22–26°C). Patch pipettes were pulled from Accu-fill 90 Micropets (Becton, Dickinson, and Co., Parsippany, NJ) coated with Sylgard (Dow Corning Corp., Midland, MI) to within 50–100 μm of their tips, and fire polished to resistances between 1.2 and 3.0 MΩ when filled with internal solution and immersed in Ringer. Membrane voltages were corrected for the junction potentials arising

between the recording pipette and the bath solution. The pipette current was nulled before seal formation (Neher, 1992). Cell membrane and pipette capacitance were canceled using electronic feedback via the patch clamp amplifier (AxoPatch 1-D, Axon Instruments Inc., Foster City, CA). A PDP-11/73 computer and interface running programs written in BASIC-23 were used to generate voltage commands and digitize and analyze patch clamp current output (Indec Systems Inc., Sunnyvale, CA). Pipette access resistance and cell capacitance were measured by analyzing the current in response to a 5-ms, 20-mV test pulse. The capacitative current transient recorded immediately after break in was fitted to a single exponential function to determine resting membrane capacitance (C_m), and initial access resistance, R_a (Lindau and Neher, 1988). Cells were selected for study if initial R_a was <10 MΩ. C_m and R_a were monitored throughout the experiment; if R_a increased more than twofold, the experiment was terminated and data from that cell excluded. The holding potential for all experiments was −60 mV. Membrane currents were measured in response to 200-ms voltage ramps from −100 to 50 mV, or 200-ms voltage pulses from the holding potential in 20-mV increments from −100 to +100 mV. Grouped data are presented as mean ± SD. When appropriate, the difference between two means was statistically tested by a two-tailed t test.

Video Microfluorescence Measurements

NIH-3T3 cells or NIH-3T3/MDR cells grown on glass coverslips were placed on the stage of an inverted microscope (Zeiss Axiovert 35). 8226 or 8226/Dox_{40} cells grown in suspension were seeded onto glass coverslips coated with poly-L-lysine (Sigma Chemical Co.). A 75 W Xenon arc lamp (Osram XBO-75), powered by a stable power supply (Model 1500, Opti-Quip Inc., Highland Mills, NY), was used as a light source. Excitation light was passed through an interference filter (470 nm, band width 20 nm for R123; and 340 nm, band width 10 nm for SPQ) and reflected by a dichroic mirror (cut-off wave lengths 505 and 400 nm, respectively, for R123 and SPQ) through a 60× plan-neofluar objective. Epifluorescence images were filtered by a barrier filter with cut-off wavelength 520/400 nm (R123/SPQ) and collected by an intensified CCD video camera (Hamamatsu, C2400). Images were digitized and averaged (8–16 frames), background-corrected, stored every 3–10 s, and analyzed by an image-processing system (VideoProbe, ETM Systems, Irvine, CA). Filters and dichroic mirrors were from Omega Optical (Brattleboro, VT). Fluorescence intensities of individual cells in the field of view (up to 512 per field) were determined by averaging the image intensity collected from regions of interest within each cell.

Imaging Plasma Membrane Chloride Conductance

Cells were loaded with SPQ by incubation in medium containing 10 mM SPQ for 2–6 h at 37°C. The intracellular SPQ concentration was ~100 μM. The fluorescence intensity of entrapped intracellular SPQ was used as a measure of halide concentration. Quenching of SPQ fluorescence by intracellular halides was determined according to the Stern-Volmer equation:

$$F = F_o/(1 + K[Hal^-]).$$

F_o and F are the SPQ fluorescence in the absence and presence of halide; $[Hal^-]$ the concentration of halide; and K a quench constant. K is equal to 118 M^{-1} for Cl^-, 276 M^{-1} for I^-, and is negligibly low for NO_3^- (Illsley and Verkman, 1987). Cells loaded with SPQ were incubated in external solution containing I^- for 20 min to quench intracellular SPQ fluorescence. When NO_3^- was exchanged for I^- in the extracellular solution, intracellular I^- ions escaped the cell through chloride channels and were replaced by NO_3^-, effectively unquenching SPQ and thereby increasing SPQ fluorescence. The rate of replacement and, hence, fluorescence increase is proportional to chloride conductance through the plasma membrane. To

study the time course of the chloride conductance, extracellular solution was toggled between solutions containing the permeant anions I^- and NO_3^-, with a period of exchange ranging from 50 to 100 s. Solution flow was propelled by 10-psi air pressure from a multibarrel tube into the experimental chamber and controlled through electromagnetic valves (General Valve, Fairfield, NJ) by VideoProbe software. Solution exchange in the 200-μl chamber was complete within <10 s. Repetitive exchange of anions in extracellular solution led to repetitive exponential decreases and increases of intracellular SPQ fluorescence as I^- and NO_3^- ions moved in and out of the cells through chloride channels. Thus, the rate of fluorescence increase and decrease was proportional to the plasma membrane chloride conductance.

Imaging P-Glycoprotein Substrate Efflux

As a substrate for extrusion by the drug-efflux pump, R123 is particularly well suited for functional investigation of P-glycoprotein (Neyfakh, 1988; Lampidis, Castello, del Giglio, Pressman, Viallet, Trevorrow, Valet, Tapiero, and Savaraj, 1989; Kessel, Beck, Kukuruga, and Schulz, 1991; Weaver, Pine, Aszalos, Schoenlein, Currier, Padmanabhan, and Gottesman, 1991; Ludescher, Thaler, Drach, Drach, Spitaler, Gattringer, Huber, and Hofmann, 1992; Altenberg et al., 1994*b*). Cells were loaded with R123 by incubation in medium containing 5 μM R123 for 20 min at room temperature. For drug-resistant cells (NIH-3T3/MDR and 8226/Dox_{40}), 5 μM verapamil was also added to block P-glycoprotein–mediated efflux of R123. After wash out of extracellular R123, the final concentration of R123 in the cells was measured by lysing $\sim 10^6$ cells in 200 μl Ringer containing 1% Triton X-100 and comparing the fluorescence intensity of the lysate with standard concentrations of R123. The average intracellular concentration of R123 was ~50 μM. External dye was washed out by rinsing the cells with $>10\times$ excess Ringer. R123 efflux was assayed by the decrease in fluorescence intensity of individual cells, and fitted with a single exponential function using Igor software (WaveMetrics, OR) run on a Macintosh (Apple Computer, Sunnyvale, CA).

RESULTS

Results are presented below in four main sections: first, a determination of molecular and functional expression of P-glycoprotein; second, patch clamp experiments demonstrating Cl^- channel opening during osmotically induced cell swelling; third, SPQ fluorescence measurements of chloride conductance in intact cells; and fourth, measurements of R123 efflux mediated by the P-glycoprotein drug-efflux pump.

Cell Phenotype

We determined the increased expression of P-glycoprotein using flow cytometry, immunofluorescence, and Western blotting. For flow-cytometric analysis, we used monoclonal 4E3 (Arceci, Stieglitz, Bras, Schinkel, Baas, and Croop, 1993) and a secondary antibody conjugated to FITC. Control NIH-3T3 mouse fibroblasts (Fig. 1 *A*) and drug-sensitive 8226 myeloma cells (Fig. 1 *C*) had identical levels of fluorescence when stained with P-glycoprotein-specific 4E3 antibody or an isotypic control. No P-glycoprotein expression was measurable in these cell lines. In contrast, compared to control, fluorescent staining was >132-fold greater in *MDR1*-transfected NIH-3T3 fibroblasts (Fig. 1 *B*) and >85-fold greater in drug-resistant 8226/Dox_{40} cells (Fig. 1 *D*) after staining with 4E3. Membranes from 8226/Dox_{40} and NIH-3T3/MDR cells contained a ~170 kD protein which was recognized by monoclonal C219. This protein was not detected in the 8226 myeloma or NIH-3T3

control cell membranes. These data confirm previously published observations that P-glycoprotein was not detectable in the drug-sensitive cell lines, but gave a strong signal in the drug-resistant cell lines when analyzed by immunoblot (Dalton et al., 1989; Tanaka, Currier, Bruggemann, Ueda, Germann, Pastan, and Gottesman, 1990). Thus, by two different criteria, the drug-resistant cells showed high levels of

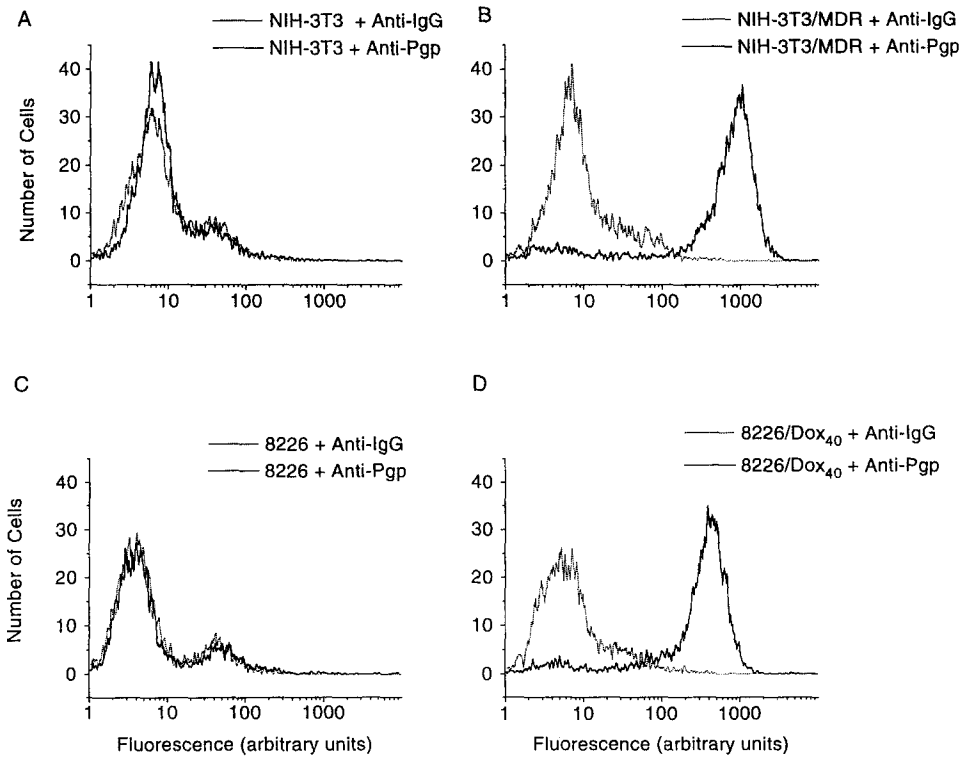

FIGURE 1. P-glycoprotein expression determined by flow cytometry. Indirect immunofluorescence from cells labeled with FITC-conjugated secondary $F(ab')_2$ fragments after incubation with an isotypic control antibody (*dotted lines*) or a P-glycoprotein-specific monoclonal antibody (4E3; *solid lines*). Drug-sensitive lines NIH-3T3 (*A*) and 8226 myeloma (*C*) and drug-resistant lines NIH-3T3/MDR (*B*) and $8226/Dox_{40}$ (*D*). Histograms plotting the number of cells against the log of the measured fluorescence show that drug-sensitive cells were equally fluorescent when labeled with control or 4E3 antibodies. In contrast, drug-resistant cells were ~100-fold more fluorescent after labeling with 4E3 compared with control. The shift in fluorescence seen for NIH-3T3/MDR cells corresponds to ~100,000 4E3 antibody-binding sites at the cell surface, according to a calibration performed with standardized fluorescent beads.

P-glycoprotein expression, while the drug-sensitive cells failed to produce measurable quantities.

To confirm that drug efflux was associated with P-glycoprotein expression in these cells, we performed dual-fluorescence measurements using a confocal microscope. R123 is a substrate for the *MDR1*-encoded drug-efflux pump (Lampidis et al., 1985; Neyfakh, 1988; Kessel et al., 1991) and mitochondrial accumulation of R123 has

been shown to be inversely correlated with multidrug resistance (Neyfakh, 1988; Ludescher et al., 1992). We incubated drug-resistant and drug-sensitive cell lines in 5 μM R123 in the presence or absence of 10 μM verapamil (Fig. 2). Verapamil reverses multidrug resistance by inhibiting drug efflux (Tsuruo, Iida, Tsukagoshi, and Sakurai, 1981; Tsuruo, Iida, Naganuma, Tsukagoshi, and Sakurai, 1983). Indirect immunofluorescence with 4E3 antibody was used to test for expression of P-

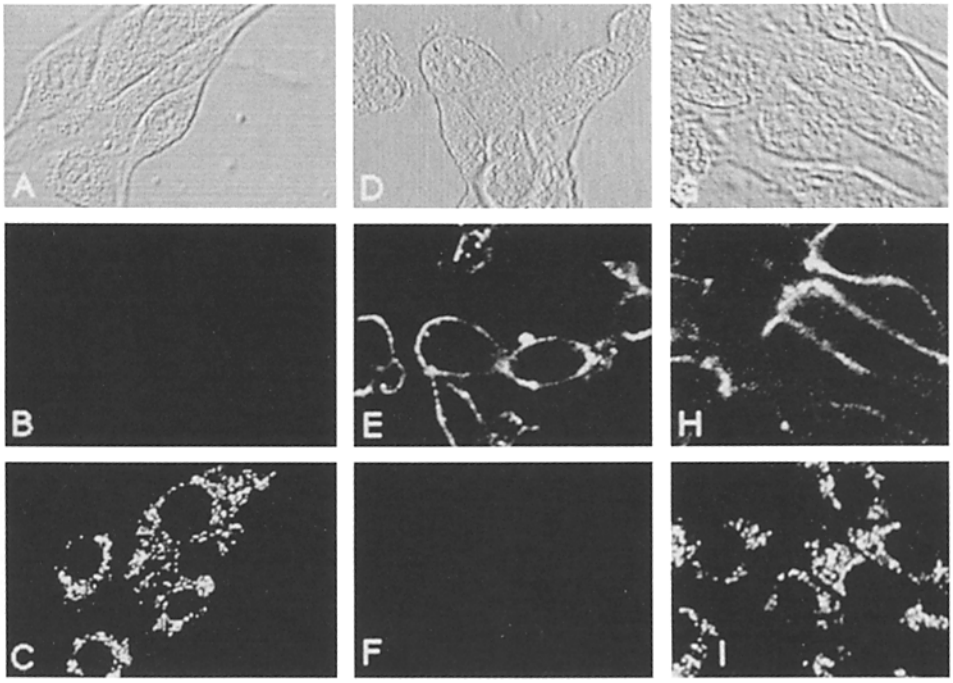

FIGURE 2. P-glycoprotein expression correlates with R123 transport. NIH-3T3 cells (*A–C*) and NIH-3T3/MDR cells (*D–I*) in nonconfocal, transmitted light images (*A,D,G*); in confocal fluorescence images showing P-glycoprotein expression by immunofluorescence (*B,E,H*); and in confocal fluorescence images showing R123 accumulation (*C,F,I*). Only the NIH-3T3/MDR cells (*E,H*) were labeled by the anti-P-glycoprotein monoclonal antibody. NIH-3T3 cells accumulated intracellular R123 after 1.5 h incubation (*C*). Punctate staining indicates mitochondrial localization of R123. No dye accumulated in NIH-3T3/MDR cells incubated in 5 μM R123 alone (*F*); however, after incubation in 5 μM R123 plus 10 μM verapamil, NIH-3T3/MDR cells showed mitochondrial accumulation of R123 (*I*) identical to the NIH-3T3 control cells (*C*).

glycoprotein during these experiments. As expected from the FACS® experiments, the drug-sensitive NIH-3T3 control cells were not labeled by 4E3 (Fig. 2 *B*), but instead showed punctate staining with R123 (Fig. 2 *C*), indicating mitochondrial localization. In contrast, NIH-3T3/MDR cell membranes were distinctly labeled by 4E3, but the cells did not accumulate R123 (Fig. 2, *E–F*). When NIH-3T3/MDR cells were incubated with R123 plus 10 μM verapamil, both membrane staining for P-glycoprotein and mitochondrial staining with R123 were observed (Fig. 2, *H–I*).

Blocking the transport function allowed R123 to enter drug-resistant cells and accumulate in the mitochondria, as seen in drug-sensitive cell lines. Similar results were obtained using this labeling protocol on 8226 myeloma and 8226/Dox_{40} cells (data not shown). Thus, drug-sensitive and drug-resistant cell lines differ both in expression of P-glycoprotein and their ability to pump R123.

Induction of g_{Cl} in Drug-sensitive and -resistant Cell Lines

In contrast to P-glycoprotein expression and drug transport, we observed no difference in the currents elicited by osmotic challenge between drug-sensitive and drug-resistant cell lines. Cell dialysis with hyperosmotic pipette solution (400 mosm) during whole-cell patch clamp experiments caused a gradual induction of an outwardly rectifying current for all four cell lines (Fig. 3). Two experiments identified

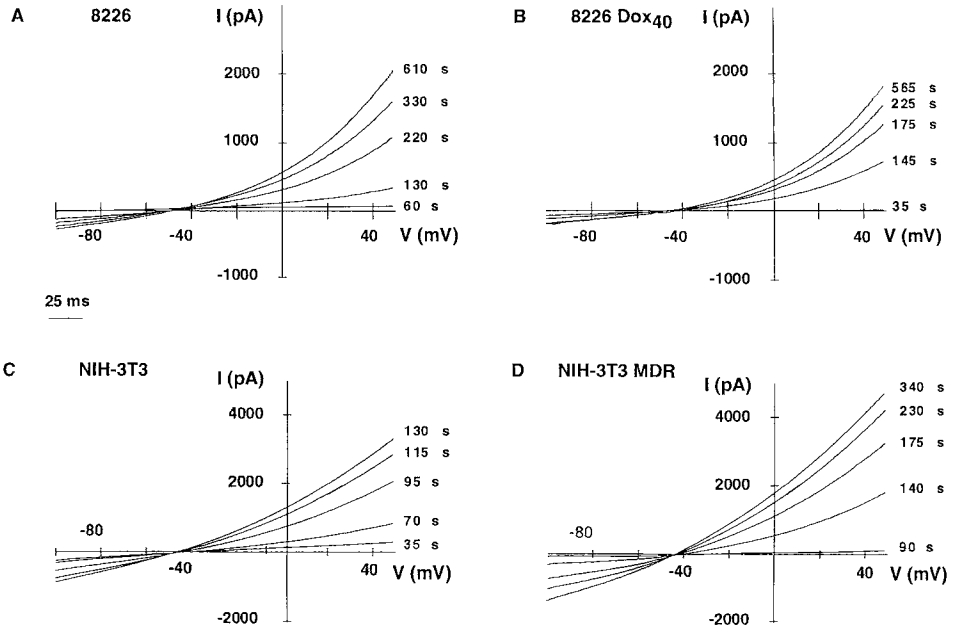

FIGURE 3. Drug-sensitive and drug-resistant cell lines express similar g_{Cl}. Dialysis with hyperosmotic cesium aspartate internal solution induced outwardly rectifying Cl^- currents in 8226-myeloma (*A*), 8226/Dox_{40} (*B*), NIH-3T3 (*C*) and NIH-3T3/MDR (*D*) cells. Whole-cell currents were elicited by 200-ms voltage ramps from −100 to +50 mV. An initial ramp was taken immediately after break in and ramps continued at 5-s intervals during dialysis. Time elapsed in seconds since break in is indicated next to each trace.

this current as a chloride current. First, when the pipette solution contained cesium and aspartate as the principal ions and the bathing solution was mammalian Ringer, the reversal potential for the current was ~ −45 mV. When most of the Ringer Cl^- was replaced by aspartate, the outward current was reduced and the reversal potential shifted to 0 mV, as expected for a chloride-selective channel (data not shown). Second, when the swelling-activated current was induced in solutions with

equivalent intracellular and extracellular Cl^- concentrations, the reversal potential was near 0 mV (see Fig. 8 below).

Using voltage-ramp stimuli, we determined the time course of Cl^- current induction by calculating the slope conductance near the reversal potential after establishing the whole-cell patch clamp configuration (break in) (Fig. 3). When currents were induced by hyperosmotic pipette solution, the conductance remained relatively constant at <1 nS for ~ 50 s and then increased over the next 200–300 s to a plateau (Fig. 4). There was no significant difference between drug-sensitive and -resistant cell lines in the maximum conductance, the rate of induction of g_{Cl}, or the reversal potential (Table I, Fig. 4). In general, the currents elicited in both NIH-3T3 fibroblast cell lines were larger than those of the paired myeloma cell lines. This difference is accounted for, in part, by the larger size of NIH-3T3 cells as measured by their membrane capacitance (Table I).

Identical Cl^- currents were induced by using isoosmotic pipette solutions (310 mosm) and challenging the cells with hypoosmotic external solutions (210 mosm) (Table I). As with the hyperosmotic stimulus, there was no difference in the maximum conductance, the rate of induction of g_{Cl}, or the reversal potential, comparing drug-sensitive with the corresponding drug-resistant cell line (Table I, Fig. 3). We also tested NMG-Cl solutions used in previous studies (Gill et al., 1992; Valverde et al., 1992), but found no difference in g_{Cl} obtained in drug-sensitive or -resistant cells. The rectification ratio ($I_{Cl,+50\ mV}/I_{Cl,-50\ mV}$) of the current in NMG-Cl solutions was 1.45 ± 0.04 ($n = 3$) for NIH-3T3 control cells and 1.46 ± 0.16 ($n = 8$) for NIH-3T3/MDR cells. These results suggest that the Cl^- channel has similar induction and permeation properties in both cell types.

Once induced, the outwardly rectifying Cl^- current was nearly constant during 200-ms voltage pulses from −100 to +100 mV, with no evidence of time-dependent channel opening or closing (Fig. 5). The current amplitudes recorded during voltage steps overlay those during voltage ramps, suggesting that outward rectification is due to permeation properties rather than voltage- or time-dependent gating. Channels slowly closed during prolonged depolarization with a time course that varied from cell to cell. During 200-ms pulses to voltages positive to +120 mV or during 10-s pulses to voltages positive to +60 mV, a slow relaxation indicating channel closure can be seen in Fig. 5. Thus, the biophysical properties of g_{Cl} did not differ between drug-sensitive and -resistant cells.

Pharmacology. The proposed link between P-glycoprotein expression and g_{Cl} was based, in part, on the argument that agents which block drug transport can also block g_{Cl}. For example, Valverde et al. (1992) showed that 100 μM verapamil, a dose that reverses multidrug resistance and prevents drug transport, decreased g_{Cl} in *MDR1*-transfected NIH-3T3 fibroblasts.

We have shown that 10 μM verapamil completely blocks the transport of R123 from 8226/Dox_{40} cells and NIH-3T3/MDR cells (see Fig. 12 below); the K_d for verapamil block is 0.3 to 0.5 μM. However, as illustrated in Fig. 6, 10 μM verapamil had no effect on g_{Cl} in NIH-3T3 control or NIH-3T3/MDR cells. Higher doses of verapamil (100 μM) reduced g_{Cl} to 70 ± 15% ($n = 3$) of control. The significantly higher concentrations required to block g_{Cl} suggest that this effect results from a different mechanism than the block of the MDR pump. In contrast, 50 μM NPPB, an anion-transport inhibitor, effectively blocked g_{Cl} (Fig. 6), but increased the rate of

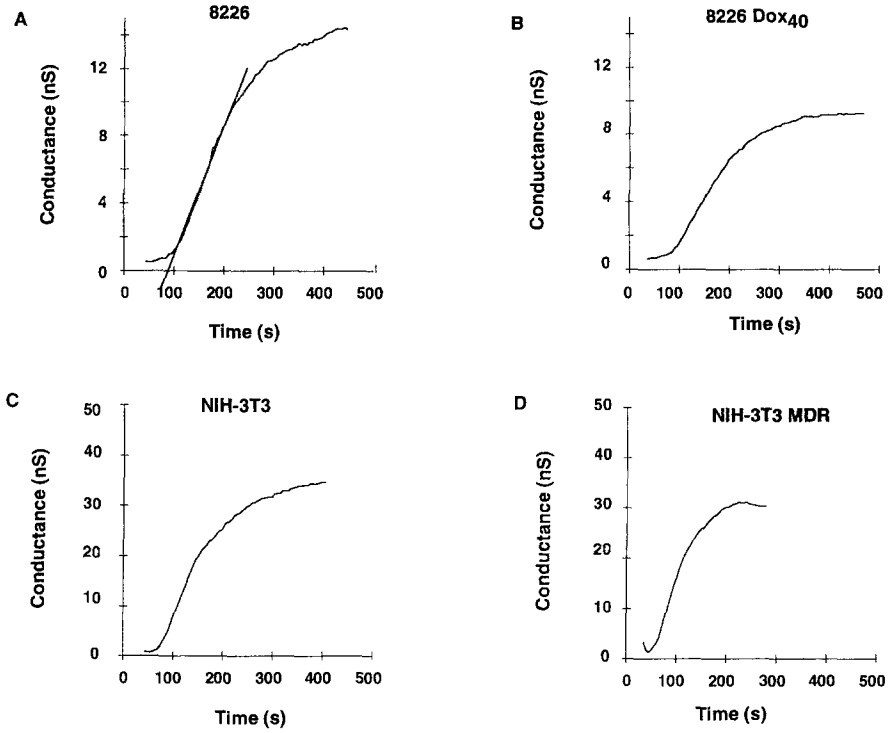

FIGURE 4. Cl^- conductance in response to osmotic challenge. The slope conductance, g_{Cl}, plotted against time after break in. Currents were elicited as described in Fig. 3; g_{Cl} was determined from a linear least-squares fit to the current-voltage relation at potentials between −35 and −55 mV. The maximal rate of increase of g_{Cl} was determined by fitting a line to the maximum slope of g_{Cl} vs time plot (e.g., straight line in *B*).

TABLE I

Induction of g_{Cl}

Cell Type	Stimulus	g_{Cl}	dg_{Cl}/dt	R_a	C_m	g_{Cl}/C_m
		nS	*nS/s*	*MΩ*	*pF*	*nS/pF*
NIH-3T3	Hypertonic internal	33.8 ± 9.1	0.24 ± 0.11	3.8 ± 0.8	29.7 ± 6.3	1.30 ± 0.31
		(*n* = 5)	(*n* = 6)	(*n* = 5)	(*n* = 5)	(*n* = 5)
NIH-3T3	Hypotonic external	25.2 ± 12.3	0.31 ± 0.30	5.3 ± 3.8	29.7 ± 6.0	0.83 ± 0.35
		(*n* = 8)	(*n* = 8)	(*n* = 8)	(*n* = 8)	(*n* = 8)
NIH-3T3/MDR	Hypertonic internal	39.4 ± 16.4	0.43 ± 0.13	4.7 ± 1.1	39.3 ± 9.2	0.99 ± 0.33
		(*n* = 6)	(*n* = 6)	(*n* = 6)	(*n* = 6)	(*n* = 6)
NIH-3T3/MDR	Hypotonic external	29.9 ± 10.9	0.52 ± 0.32	4.4 ± 4.2	36.6 ± 5.9	0.82 ± 0.30
		(*n* = 23)	(*n* = 25)	(*n* = 22)	(*n* = 22)	(*n* = 22)
8226	Hypertonic internal	6.1 ± 3.8	0.03 ± 0.02	4.9 ± 1.0	21.5 ± 4.9	0.31 ± 0.20
		(*n* = 12)	(*n* = 12)	(*n* = 9)	(*n* = 9)	(*n* = 9)
8226/Dox_{40}	Hypertonic internal	7.7 ± 5.3	0.03 ± 0.02	4.6 ± 1.0	21.2 ± 7.2	0.37 ± 0.22
		(*n* = 10)	(*n* = 8)	(*n* = 7)	(*n* = 7)	(*n* = 7)

Cell swelling was induced by addition of 100 mM sucrose to the pipette solution or by exchange of the bathing solution with 67% Ringer. g_{Cl} and dg_{Cl}/dt were calculated from the slope of the *I–V* relation near the reversal potential for currents elicited by ramp stimuli as in Fig. 5. R_a and C_m were calculated as described in the Methods. When g_{Cl} was normalized for the size of the cell (g_{Cl}/C_m), there was no significance in the magnitude or rate of induction of g_{Cl} in either drug-sensitive and -resistant cell pair. Data are presented as the mean ± SD.

R123 transport (see Fig. 13 below). The chloride-channel blocker, DIDS (50 μM) blocked g_{Cl} in both NIH-3T3 control and NIH-3T3/MDR cells (Figs. 6 and 7), whereas doses as high as 1 mM had little effect on R123 transport (see Fig. 13 below). All three compounds had similar effects on g_{Cl} in 8226 myeloma and 8226/Dox_{40} cells (data not shown). Thus, our results demonstrate that verapamil blocks drug transport at doses that have no effect on g_{Cl}. Conversely, DIDS blocks the current at doses which do not affect drug transport. Finally, NPPB can block the current at doses that increase drug transport.

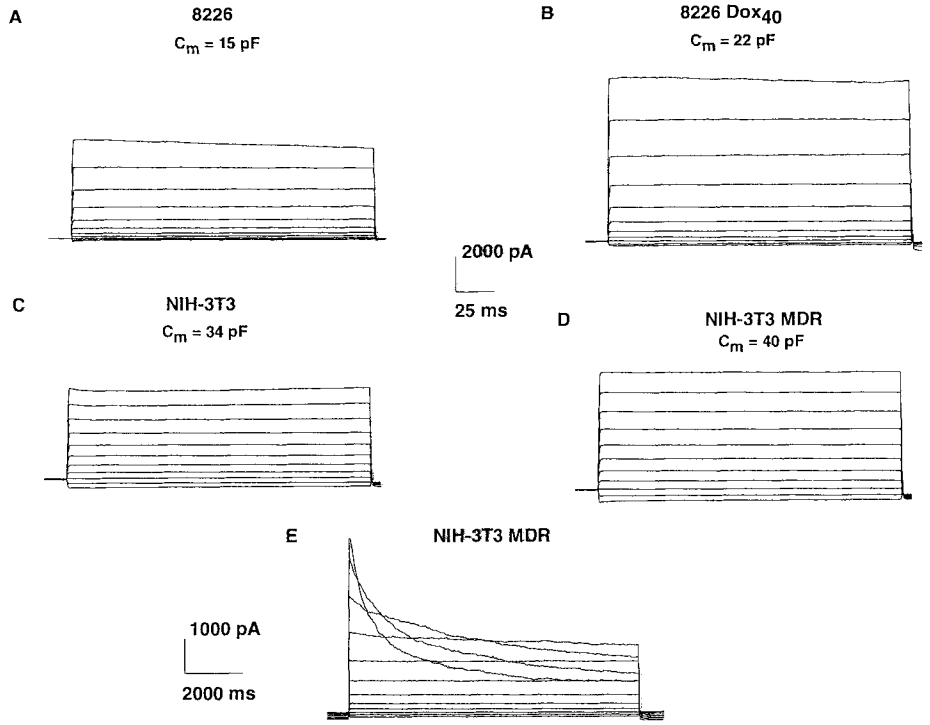

FIGURE 5. Cl^- currents elicited by a series of 200-ms voltage pulses from −100 to +100 mV. Internal solution: hyperosmotic Cs aspartate; external solution: mammalian Ringer. Currents were neither leak-subtracted nor normalized for cell size. For all cells, I_{Cl} had similar magnitude and kinetics. The larger currents in 8226/Dox_{40} and NIH-3T3/MDR cells (*B* and *D*) can be accounted for by cell size, as indicated by measured C_m values (see Table I). 200-ms pulses over this voltage range resulted in little or no channel closing. (*E*) During prolonged depolarizations up to +120 mV, slow channel closing may be seen for voltage pulses > +60 mV.

According to the dual-function model for P-glycoprotein, substrate binding to the drug transporter should inhibit drug transport (Gill et al., 1992). We tested this prediction during whole-cell patch clamp experiments by dialyzing the cell with 200 μM doxorubicin before exposure to hypoosmotic external solution. Since doxorubicin is fluorescent, we confirmed its intracellular dialysis by video imaging: half times for dialysis ranged from 150–300 s depending on R_a. When fluorescence had reached a steady state, we exchanged the bath solution with 70% Ringer, effecting cell swelling

and the subsequent characteristic induction of outwardly rectifying Cl^- current (Fig. 8). In 17 similar experiments, neither the amplitude of g_{Cl} nor its rate of induction after hypoosmotic swelling was altered by 200 μM doxorubicin or 250 μM vincristine in the pipette solution (Fig. 9 and Table II).

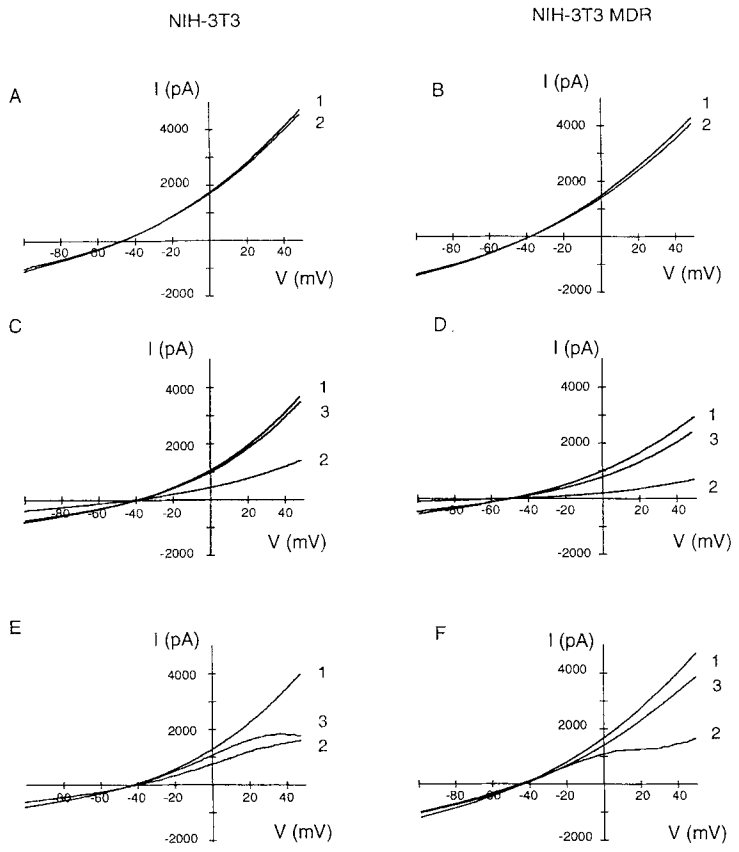

FIGURE 6. Pharmacological effects on volume-activated g_{Cl}. Voltage ramps were used to test the effects of verapamil (*A,B*), NPPB (*C,D*) and DIDS (*E,F*) on g_{Cl} in NIH-3T3 (*A,C,E*) and NIH-3T3/MDR (*B,D,E*) cells. In each case, traces are labeled as 1 (control), 2 (drug), and 3 (wash out). Verapamil, at a dose (10 μM) that completely blocks R123 efflux (see text), did not affect g_{Cl}. Conversely, 50 μM NPPB and DIDS significantly reduced g_{Cl} in both drug-sensitive and drug-resistant cells. DIDS had no effect on R123 transport and NPPB actually increased the apparent rate of R123 transport.

Swelling-activated Chloride Conductance in Intact Cells

Our initial observations using whole-cell recording provided no support for the hypothesis that P-glycoprotein can function in a dual manner (Gill et al., 1992). To address this issue by an independent method, one that could be applied to intact cells, we used a video-imaging fluorescence-quench assay to monitor membrane chloride permeability (see Materials and Methods). Under isoosmotic conditions, there

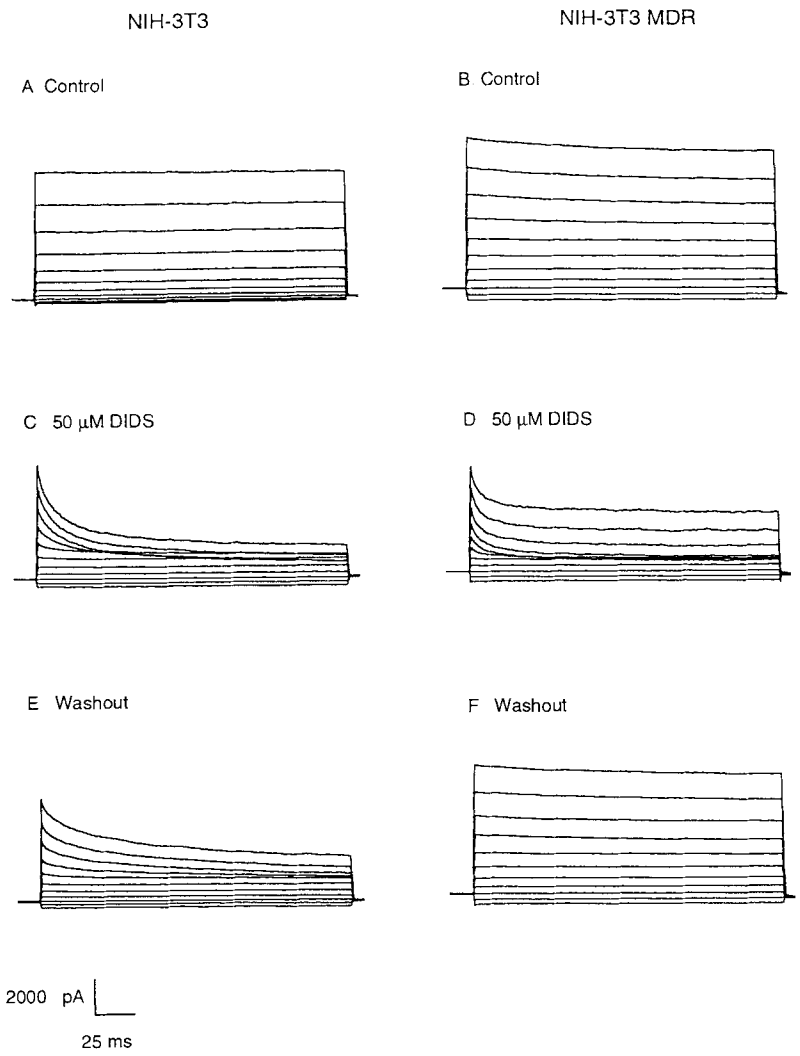

FIGURE 7. DIDS blocks g_{Cl}. Cl^- currents were recorded before, during, and after application of 50 μM DIDS. Currents were evoked by 200-ms voltage steps from −100 to +100 mV in 20-mV steps from a holding potential of −60 mV. Cells were first bathed in normal Ringer, then hypoosmotic Ringer to induce g_{Cl} (not shown); the internal solution was isoosmotic CsAsp. DIDS was applied in hypoosmotic Ringer. DIDS blocked the current induced in NIH-3T3 control or NIH-3T3/MDR cells in a time- and voltage-dependent manner; block was partially reversed by a return to drug-free hypoosmotic Ringer. The degree of block and the recovery from block was variable for both the drug-sensitive and -resistant cell lines. Long incubations with higher concentrations of DIDS resulted in irreversible block.

was little g_{Cl} activated, and little or no increase of SPQ fluorescence due to I^-/NO_3^- exchange. Induction of g_{Cl} by swelling the cells with hypoosmotic extracellular solution (67% of isoosmotic) led to a rise in SPQ fluorescence that could be fitted by a single-exponential function (Fig. 10*A*). The rate of this rise was a measure of

chloride conductance at the time of osmotic challenge. Osmotically induced cell swelling increased g_{Cl} in both drug-sensitive and -resistant cells (Fig. 10, *B–E*). Measurement of SPQ fluorescence from each individual cell in the microscopic field of view enabled a stimulus-response relationship between chloride conductance and cell swelling to be determined in separate experiments using drug-sensitive or -resistant cells. The threshold of the increase in the SPQ signal, and hence the chloride conductance, ranged from 80 to 70% of initial osmolarity. Although the

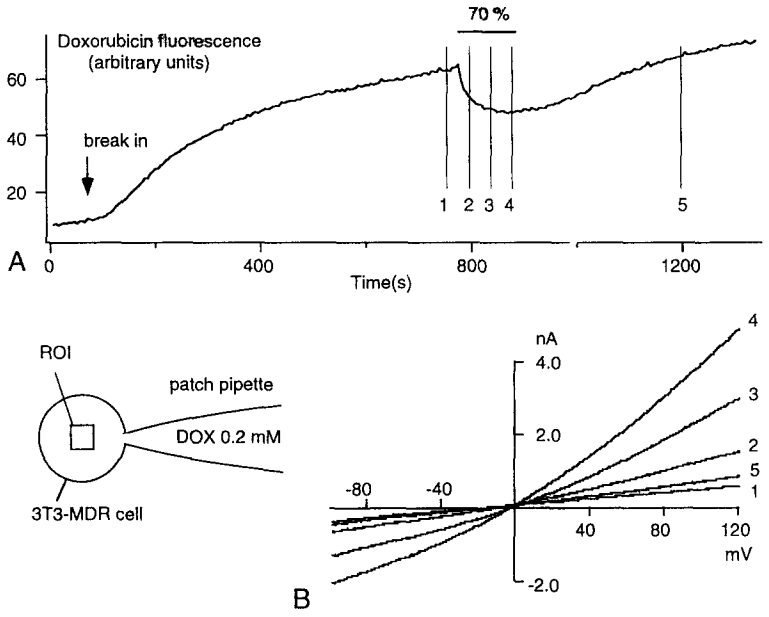

FIGURE 8. Swelling-activated chloride currents were not affected by doxorubicin. When 200 μM doxorubicin was included in the isotonic pipette solution, its entry into the cell could be monitored by measuring the fluorescence in a region (ROI) near the center of cell as shown in the inset diagram. (*A*) shows the increase in cellular fluorescence due to the dialysis of the cell with doxorubicin. In four experiments of this type, with pipette access resistances ranging from 2.8 to 9 MΩ, half times for dialysis ranged from 150 to 300 s. As the fluorescence intensity approached a steady state, the cell was swollen by exposure to hypoosmotic media (*70% bar*). A series of voltage ramps was applied to the cell before (*1*), during (*2–4*), and after (*5*) exposure to hypoosmotic Ringer. (*B*) The currents elicited by the voltage ramps show a clear induction of g_{Cl} during exposure to hypoosmotic Ringer (*1–4*). This current was reversed upon return to isotonic Ringer (*5*). Pipette solution: isoosmotic NMGCl internal solution. Bath solutions: isoosmotic NMGCl Ringer followed by hypoosmotic NMGCl Ringer.

maximal amplitude of swelling-activated chloride conductance was virtually indistinguishable in both cell types, the threshold for chloride channel opening varied from batch to batch, depending upon the time of cell passage, and between sensitive and resistant cell lines. Under identical conditions, drug-resistant cells (NIH-3T3/MDR) had a somewhat lower threshold (Fig. 10 *F*); this difference was more pronounced early after cell passage.

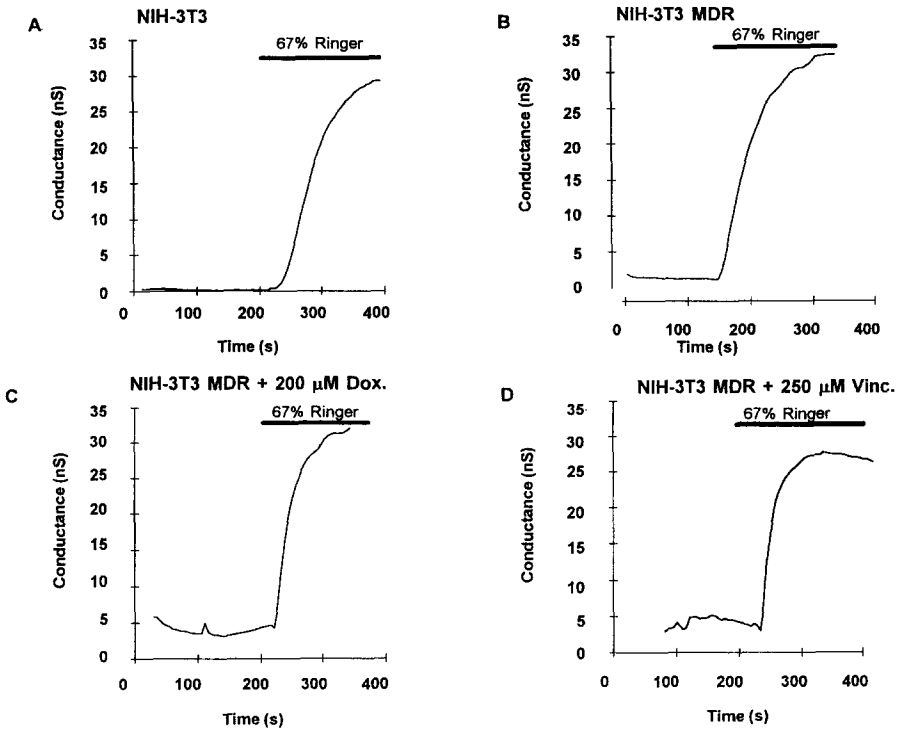

FIGURE 9. g_{Cl} induction is not affected by cell dialysis with doxorubicin or vincristine. When NIH-3T3 (*A*) or NIH-3T3/MDR (*B*) cells were dialyzed with isotonic pipette solution, g_{Cl} remained at a very low level for more than 200 s. At this time, dialysis directly monitored from the fluorescence of doxorubicin was roughly 50% complete. Exchanging isotonic Ringer solution bathing the cells with hypoosmotic Ringer (67% bar) increased g_{Cl} with or without drug. Chloride conductance was measured as described in Fig. 4. Inclusion of 200 μM doxorubicin (*C*) or 250 μM vincristine (*D*) in the pipette solution did not affect the magnitude or the rate of increase of g_{Cl} in NIH-3T3/MDR cells. The leakage conductance of the cell in isoosmotic solution was often increased during dialysis with either vincristine or doxorubicin.

TABLE II

Substrates of the Drug-Efflux Pump Do Not Affect g_{Cl}

Cell Type	Drug	g_{Cl}	dg_{Cl}/dt	R_a	C_m	g_{Cl}/C_m
		nS	*nS/s*	*MΩ*	*pF*	*nS/pF*
3T3/MDR	Control	29.9 ± 10.9	0.52 ± 0.32	4.4 ± 4.2	36.6 ± 5.9	0.83 ± 0.31
		(*n* = 23)	(*n* = 25)	(*n* = 22)	(*n* = 22)	(*n* = 22)
3T3/MDR	250 μM vincristine	31.4 ± 9.7	0.62 ± 0.46	4.0 ± 1.4	30.6 ± 8.4	1.03 ± 0.16
		(*n* = 4)	(*n* = 4)	(*n* = 4)	(*n* = 4)	(*n* = 4)
3T3/MDR	200 μM doxorubicin	33.4 ± 10.9	0.57 ± 0.28	5.3 ± 3.7	47.4 ± 14.4	0.73 ± 0.24
		(*n* = 6)	(*n* = 6)	(*n* = 6)	(*n* = 6)	(*n* = 6)
8226/Dox_{40}	Control	7.7 ± 5.3	0.03 ± 0.02	4.6 ± 1.0	21.2 ± 7.2	0.50 ± 0.34
		(*n* = 10)	(*n* = 8)	(*n* = 7)	(*n* = 7)	(*n* = 7)
8226/Dox_{40}	200 μM doxorubicin	6.0 ± 5.9	0.04 ± 0.05	4.7 ± 1.1	15.7 ± 3.8	0.34 ± 0.25
		(*n* = 7)	(*n* = 7)	(*n* = 7)	(*n* = 7)	(*n* = 7)

Drugs were included in the pipette solution and dialyzed into the cells for 200 s before g_{Cl} was induced by cell swelling. Data are presented as the mean ± SD.

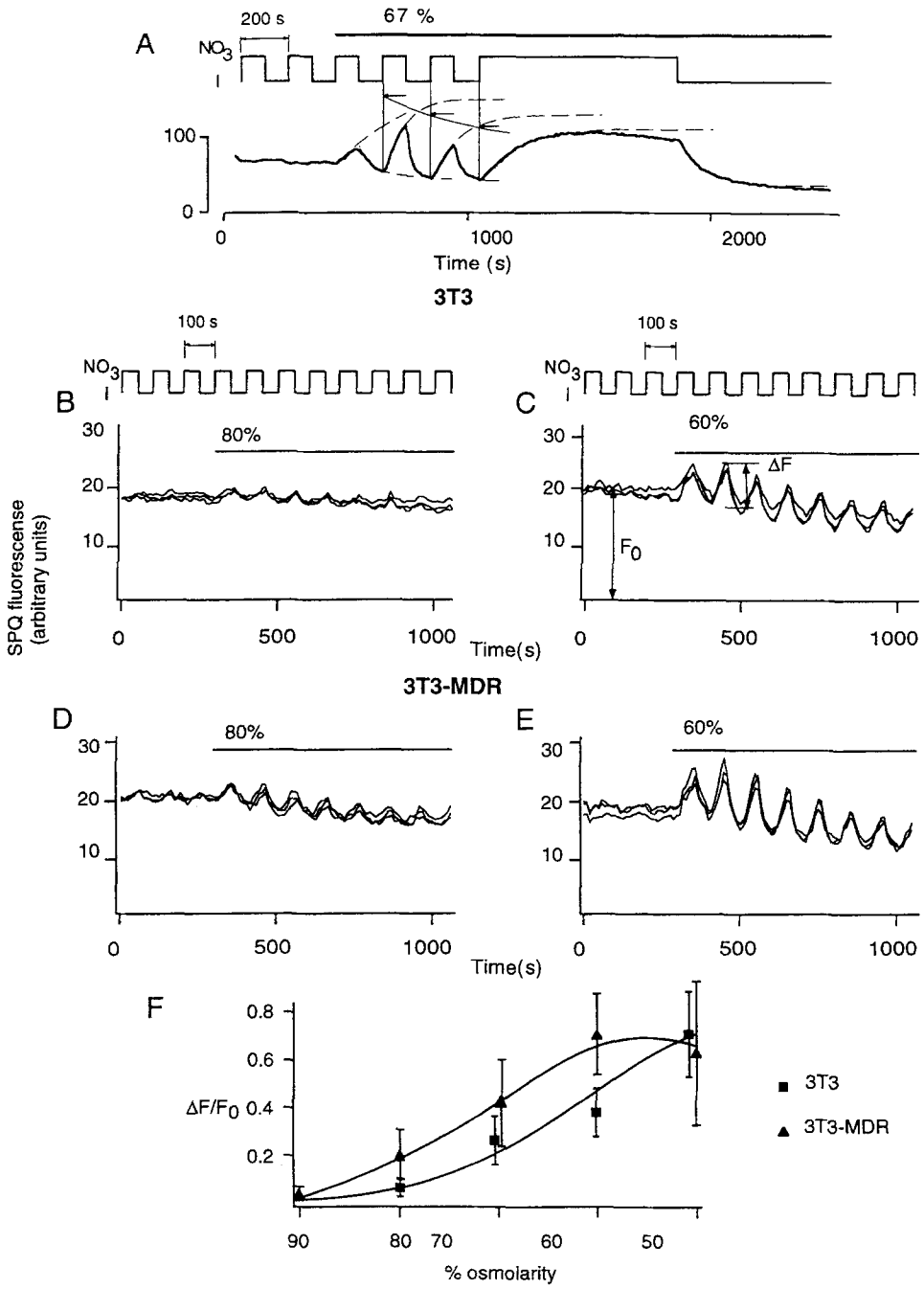

FIGURE 10. SPQ-fluorescence assay of transmembrane chloride conductance in intact cells. (*A*). Changes in SPQ fluorescence in NIH-3T3 cells. Initially, the fluorescence was quenched by preincubating the cells in extracellular solution containing I^-. At first, chloride conductance is small, so I^-/NO_3^- replacement does not lead to an immediate increase in fluorescence.

Pharmacology. The sensitivity of g_{Cl} to various pharmacological agents in intact cells is illustrated in Fig. 11. Verapamil, which blocks P-glycoprotein-associated drug efflux at submicromolar concentration, had little or no effect on g_{Cl}. Among several agents tested, the most effective blocker was tamoxifen; 10 μM completely and irreversibly blocked the conductance after ~100 s. DIDS and NPPB quickly and reversibly blocked the conductance at concentrations of 1 mM and 30 μM, respectively. Our SPQ-quench measurements of g_{Cl} corroborate the patch clamp data; in comparison with R123 efflux measurements (below), both methods of measuring g_{Cl} demonstrate that the swelling-activated chloride channel and the P-glycoprotein-mediated drug efflux pump have very different pharmacological sensitivities.

R123 Efflux in Drug-sensitive and -resistant Cells

The first section of Results used steady state levels of R123 accumulation to document P-glycoprotein levels in drug-resistant cell lines. Here, we describe the rates of R123 efflux measured from the decrease in R123 fluorescence after removing extracellular dye. The time course demonstrates that the rate of R123 efflux in 8226/Dox_{40} cells is nearly 100 times higher than in the drug-sensitive counterpart, 8226 (Fig. 12). Verapamil is a highly effective inhibitor of P-glycoprotein–mediated multidrug resistance, and blocked P-glycoprotein-mediated R123 efflux (Fig. 12 *A*). In the control cells, verapamil had no effect (Fig. 12 *B*). To study the dose dependence of verapamil block, we measured the decrease in R123 fluorescence in the presence of varying concentrations of verapamil (Fig. 12 *C*). The concentration dependence was fitted with the equation:

$$1/\tau = (1/\tau_o) * 1/(1 + [ver]/K_d) + 1/\tau_v,$$

where τ is a time constant for the decrease in R123 fluorescence, τ_o the time constant in the absence of verapamil, τ_v the time constant at saturating concentrations of verapamil, [ver] the verapamil concentration, and K_d the binding constant for

---

Hypoosmotic challenge (67%) activates g_{Cl} leading to an increase in the rate of SPQ fluorescence rise. NO_3^-/I^- pulsing with a period of 100/100 s. Quenching and unquenching of SPQ fluorescence was fitted with a single exponential function. There was also a slow, irreversible decrease in SPQ fluorescence (indicated by arrows in *A*), apparently due to leak of SPQ from the cell, which was further facilitated by osmotic challenge. The time constant of this leak was ~600 s and was taken into account during prolonged experiments. During the first 100 s after solution exchange, the time dependence of SPQ fluorescence was close to linear and the simple ratio of maximal fluorescence over initial fluorescence ($\Delta F/F_o$) could be used as a measure of membrane chloride conductance. Therefore, we used short pulses (50/50 s) of solution to measure g_{Cl}. Arrows indicate upper limits of SPQ fluorescence that would be reached after NO_3^- application. Fluorescence measurements for three cells are shown in each of panels (*B–E*). The bar indicates hypoosmotic/isoosmotic Ringer exchange. Reducing osmolarity to 80% (*B,D*) caused a small increase of g_{Cl} in NIH-3T3 control cells and a slightly larger increase in NIH-3T3 MDR cells. 60% Ringer (*C,E*) induces a larger change in g_{Cl} in NIH-3T3 control cells and in NIH-3T3 MDR cells. (*F*) Stimulus-response of Cl^- conductance vs osmolarity. Values represent mean ±SD for g_{Cl} for NIH-3T3 control (n = 37) and NIH-3T3 MDR (n = 42) cells. Thus, drug-resistant and -sensitive cells had the same maximal g_{Cl}, but drug-resistant cells had a slightly higher sensitivity to osmotic challenge.

verapamil. The K_d for blocking R123 efflux from 8226/Dox$_{40}$ cells was 0.54 μM. Similar results were obtained in NIH-3T3/MDR cells (K_d of 0.39 μM, data not shown).

Cl^--channel blockers do not inhibit R123 efflux. Patch clamp studies presented above show that swelling-activated chloride channels in drug-resistant and drug-sensitive 3T3 fibroblasts and 8226 myeloma cells are blocked by DIDS, tamoxifen,

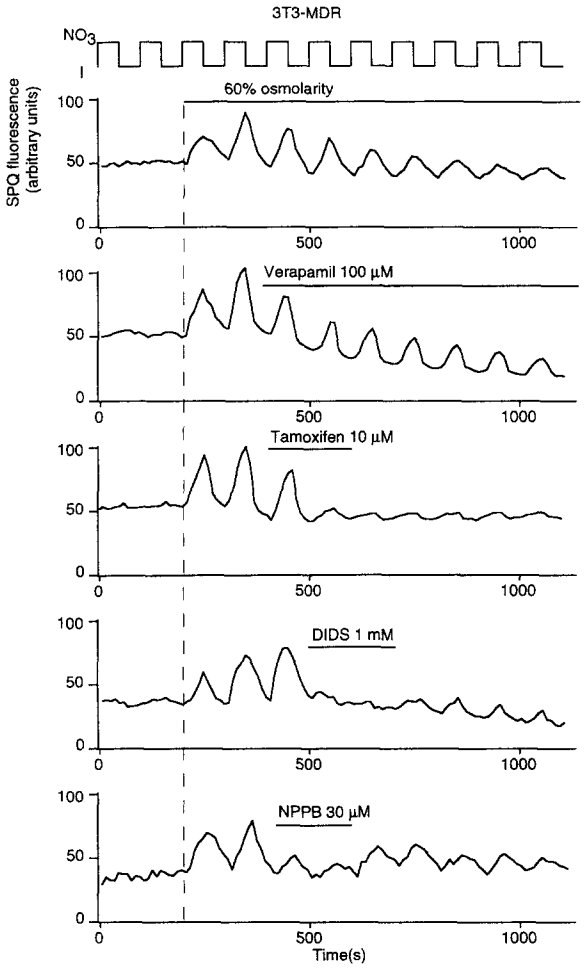

FIGURE 11. Effects of verapamil, tamoxifen, DIDS, and NPPB on g_{Cl} in NIH-3T3 MDR cells superfused with 60% Ringer. Panels show averaged SPQ fluorescence signals for 27–42 cells. Top shows a control response. Verapamil (100 μM) had no significant effect on g_{Cl}. Tamoxifen (100 μM) slowly ($t_{1/2}$ = 100 s) and irreversibly blocked g_{Cl}. DIDS (1 mM) and NPPB (30 μM) caused a rapid ($t_{1/2}$ < 10 s) and reversible reduction in g_{Cl}. DIDS fluorescence has considerable spectral overlap with SPQ; to compensate for variations in background fluorescence we subtracted background fluorescence measured in regions of interest positioned near each individual cell from the cells' fluorescence.

and NPPB. Inhibition was confirmed in intact cells using the SPQ fluorescence assay (Fig. 11). None of these blockers inhibited P-glycoprotein-mediated R123 efflux (Fig. 13, *A–C*). These results demonstrate that pumping can occur normally even though Cl^- channel function is completely blocked.

Mitochondrial uncouplers accelerate R123 efflux. The chloride-channel blocker, NPPB, markedly increased the rate of R123 efflux in drug-resistant cells (Fig. 13 *D*).

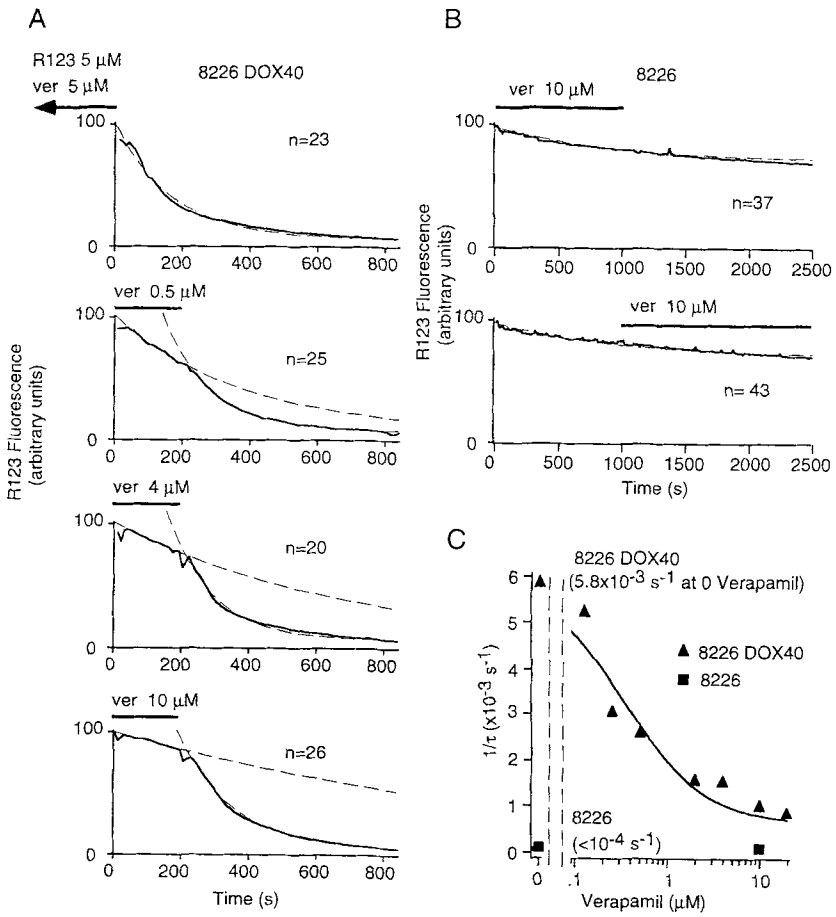

FIGURE 12. Rhodamine-123 efflux differs between 8226/Dox_{40} (*A*) and 8226 myeloma cells (*B*). Cells were loaded by incubation with 5 μM R123 and 5 μM verapamil (*ver*) for 20 min. The cells were washed with Ringer containing the indicated concentration of verapamil at 0 s, and were washed with drug-free Ringer at 200 s. Fluorescence intensity was used as a measure of intracellular R123 concentration. Each panel is an average of the traces from the indicated number of cells. (*A*) The rate of R123 efflux was determined by fitting exponential functions to the decrease of fluorescence with time. In the absence of verapamil (*A, top*), the trace was fitted with a single-exponential function. For the remaining panels, the trace was divided into two parts (from 0 to 200 s in the presence of verapamil; and from 200 s to 850 s after washout of verapamil), and each part was separately fitted by a single exponential function. This analysis gave the rate of efflux of R123 in presence and absence of verapamil. Verapamil caused a dose-dependent decrease in the rate of R123 efflux. After washout of verapamil, the rate of R123 efflux did not differ significantly from control. (*B*) In control, 8226 cells, the decline of R123 fluorescence is extremely slow and unaffected by verapamil added either early or late in the experiment. (*C*) The rate of R123 efflux is plotted against the log of the dose of verapamil for both cell types.

This result was initially surprising, but can be explained by the ability of NPPB to increase the cytoplasmic concentration of R123 by redistributing the substrate inside the cells. R123 is positively charged and accumulates primarily in mitochondria (Fig. 14); the cytoplasmic concentration is much lower because the mitochondrial membrane potential allows the positively charged dye to be sequestered (Neyfakh, 1988; Lampidis et al., 1989; Weaver et al., 1991). It has been shown that NPPB, besides being a Cl^- channel blocker, uncouples oxidative phosphorylation in mitochondria and increases the proton permeability of the plasma membrane in phagocytic cells

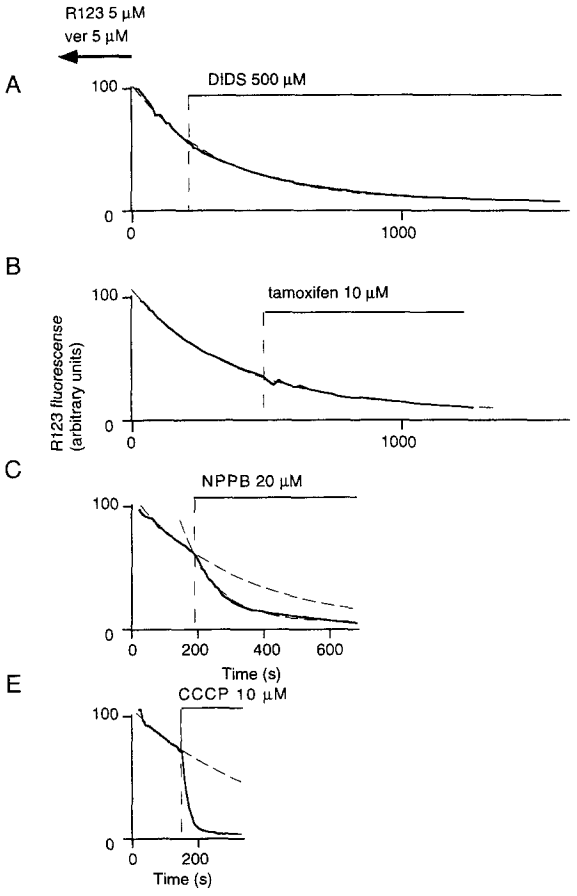

FIGURE 13. Chloride-channel blockers have differing effects on R123 efflux. Time course of R123 efflux from NIH-3T3 MDR cells was measured as described in Fig. 12. The addition of DIDS (*A*) or tamoxifen (*B*) had no significant effect on the rate of R123 efflux. NPPB (*C*) and CCCP (*D*) significantly increased the rate of R123 efflux. Traces shown are the average of 27–39 cells. Rates of efflux were determined by the fit of two individual single-exponential functions before and after drug addition. Neither CCCP nor NPPB increased the rate of R123 efflux in drug-sensitive control NIH-3T3 and 8226 cells (data not shown). Moreover, neither CCCP nor NPPB overcame the blocking effect of verapamil on R123 efflux in drug-resistant cells (data not shown).

(Lukacs, Nanda, Rotstein, and Grinstein, 1991). An uncoupler would decrease the electrochemical gradient across the mitochondrial membrane, causing R123 release to the cytoplasm, thus making the dye more accessible to the P-glycoprotein-associated pump in the plasma membrane.

We confirmed the uncoupling action of NPPB by demonstrating that NPPB causes changes in the pattern of R123 fluorescence in NIH-3T3 cells. Confocal microscopy images taken before adding NPPB revealed R123 fluorescence within mitochondria, with little or no nuclear staining; after adding NPPB, the fluorescence became evenly

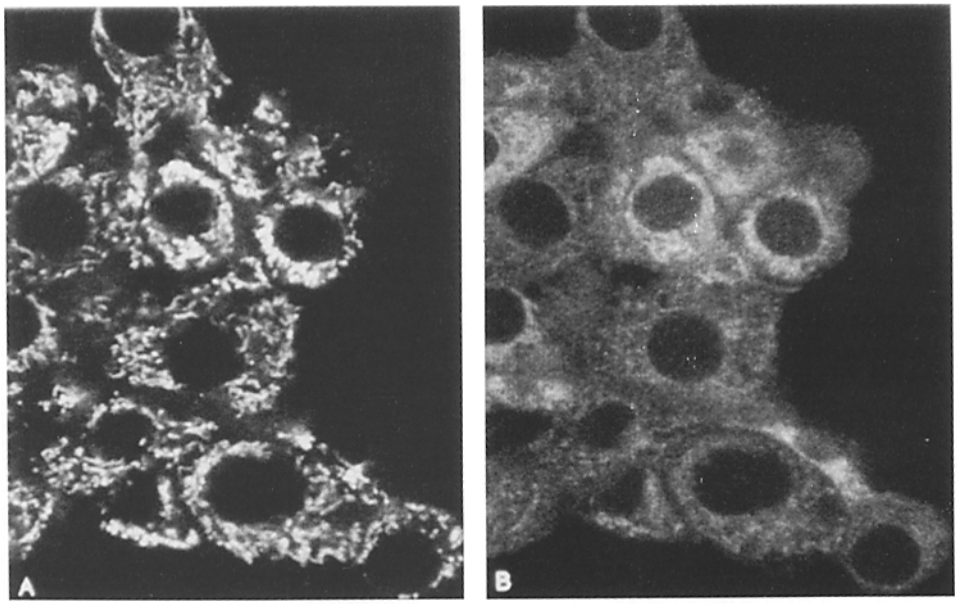

FIGURE 14. NPPB releases R123 from mitochondria. (*A*) Confocal images of NIH-3T3/MDR cells loaded with R123 in the presence of 10 μM verapamil display bright, punctate staining of mitochondria. (*B*) Images taken 100 s after adding NPPB show more diffuse staining with R123. The integral of the fluorescence intensity over each individual cell was not significantly different before or after addition of NPPB. Similar results were obtained with NIH-3T3 control cells and with both cell lines using CCCP instead of NPPB (data not shown).

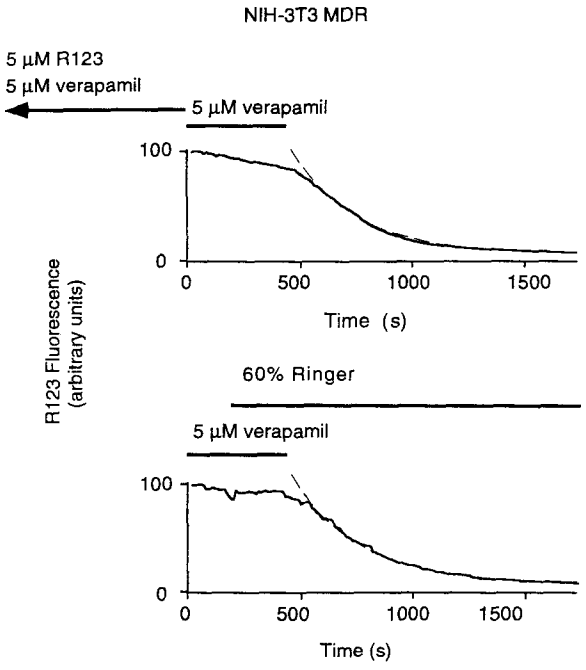

FIGURE 15. Cell swelling does not affect R123 efflux. Cells were swollen by applying 60% Ringer, causing a large increase in g_{Cl} (see Fig. 10). R123 efflux was measured as described in Fig. 12. Rates of efflux were not significantly different in control experiments (*A*) and when NIH-3T3 MDR cells were swollen with 60% Ringer (*B*). Traces in *A* and *B* are averages from 37 and 32 cells, respectively.

distributed throughout the cytoplasm, with considerable nuclear staining (Fig. 14). As expected from results with NPPB, extracellular application of another protonophore, carbonyl cyanide *m*-chlorophenylhydrazone (CCCP) causes redistribution of mitochondrial R123, along with a rapid collapse of the mitochondrial electrochemical gradient. In cells expressing P-glycoprotein, CCCP causes a dramatic increase in the rate of R123 efflux (Fig. 14 *E*). We conclude that the normal rate of R123 efflux observed in the absence of uncoupler is limited by the rate of release from mitochondria.

R123 efflux is not blocked by cell swelling. It has been proposed that the swelling-activated chloride conductance is mediated by P-glycoprotein, with P-glycoprotein functioning either as a chloride channel during cell swelling or a drug-efflux pump (Valverde et al., 1992). This model implies that activation of g_{Cl} would impair drug pumping by drug-resistant cells. However, the measured time constants for R123 efflux were 314 ± 19 s (n = 37) in isoosmotic Ringer and 328 ± 23 s (n = 32) in 60% Ringer in NIH-3T3/MDR cells (Fig. 15). Similar results were obtained in three additional experiments on 3T3/MDR cells and two experiments on 8226/Dox_{40} cells. Thus, R123 extrusion was not significantly different in cells swollen by hyposmotic extracellular solution.

DISCUSSION

In this study, we examined the hypothesis that P-glycoprotein forms swelling-activated Cl^- channels. Our principal aim was to determine if P-glycoprotein expression affected the magnitude or biophysical properties of g_{Cl} in drug-sensitive and -resistant cells. Indirect immunofluorescence and confocal microscopy demonstrated that membrane localization of P-glycoprotein accompanied the multidrug-resistant phenotype. Video imaging showed that unidirectional R123 efflux, a measure of P-glycoprotein function, was significantly higher in drug-resistant cells. Using two independent and complementary assays of g_{Cl}, whole-cell current recording and SPQ-fluorescence quench, we showed that cell swelling induced the same level of chloride conductance in the drug-sensitive and -resistant cells. In addition, comparing the dose dependence for inhibition of g_{Cl} and R123 transport clearly dissociates the pharmacology of block for drug transport and chloride conductance. Furthermore, we tested two predictions of a model proposing that P-glycoprotein acts exclusively as a transport pump or an ion channel (Gill et al., 1992). Contrary to the model's predictions, we find that induction of swelling-activated chloride channels does not inhibit R123 efflux, and R123 efflux does not inhibit g_{Cl} in drug-resistant cells. Thus, these two processes appear to occur independently.

Biophysical Properties of g_{Cl} in Drug-sensitive and -resistant Cells

In drug-sensitive and -resistant NIH-3T3 fibroblasts or 8226 myeloma cells, I_{Cl} exhibited moderate outward rectification in symmetrical chloride solutions, slow and somewhat variable closing kinetics during long pulses to voltages positive to +60 mV, and similar K_d values for block by DIDS, NPPB, and tamoxifen. The rectification ratio of I_{Cl} and the relative permeabilities of chloride, aspartate, and glutamate were identical in all four cell lines. The induction of g_{Cl} in response to cell dialysis with

hyperosmotic pipette solution, or bath exchange with hypoosmotic Ringer, occurred over the same time course for both drug-sensitive and -resistant cells. During whole-cell recording, the maximum g_{Cl} varied with the size of the cell, but not with the level of expression of P-glycoprotein. Thus, electrophysiological measurements do not distinguish between g_{Cl} in these cells.

Swelling-activated Cl^- channels have now been observed in a wide variety of cell types (reviewed in Cahalan and Lewis, 1994). Indeed, in our experience it has been difficult to find a cell type in which g_{Cl} does not activate when swollen during whole-cell recording by an imposed osmotic gradient. The control drug-sensitive NIH-3T3, myeloma, and MCF-7 cell lines lacking P-glycoprotein are no exception. Based on biophysical characteristics, swelling-activated Cl^- channels may be divided into two classes: a small conductance channel that closes very slowly during strong depolarization, and a larger conductance channel that closes more rapidly during strong depolarization. Lymphocytes, chromaffin cells, neuroblastoma cells, neutrophils, fibroblasts, osteoclasts, cardiac cells, endothelial cells and *Xenopus* oocytes have channels that are activated by swelling, show moderate outward rectification in symmetrical chloride solutions, and lack voltage-dependent gating (Estacion, 1991; Tseng, 1992; Falke and Misler, 1989; Lewis et al., 1993; Doroshenko and Neher, 1992; Pollard, 1993; Stoddard, Steinbach, and Simchowitz, 1993; Zhang, Rasmusson, Hall, and Lieberman, 1993; Kelly, Dixon, and Sims, 1994; Nilius, Oike, Zahradnik, and Droogmans, 1994; Ackerman, Wickman, and Clapham, 1994). A single-channel conductance of 1–2 pS was estimated by fluctuation analysis of whole-cell currents in T lymphocytes, neutrophils and endothelial cells (Cahalan and Lewis, 1988; Lewis et al., 1993; Stoddard et al., 1993; Nilius et al., 1994). In epithelial cells from the airway and trachea, intestinal or colon cells, and Ehrlich ascites tumor cells, single-channel conductances of 28–75 pS have been measured (Worrell, Butt, Cliff, and Frizzell, 1989; Solc and Wine, 1991; Kubo and Okada, 1992; Christensen and Hoffmann, 1992). Several epithelial cell lines have volume-sensitive Cl^- channels that close at voltages positive to +80 mV (Worrell et al., 1989; Solc and Wine, 1991; Kubo and Okada, 1992; Rasola, Galietta, Gruenert, and Romeo, 1992). The time course of closing appears to be one of the most variable properties of these channels. For example, in T_{84} cells, closing time constants range from several hundred ms (Solc and Wine, 1991) to several seconds (Worrell et al., 1989). Slow channel closing was observed with variable kinetics in our experiments on NIH-3T3 cells (e.g., Fig. 5 *E*). The widespread expression of swelling-activated chloride currents and the variability in their biophysical properties (single-channel conductance, permeability ratios, and closing) suggest that these channels comprise a large and complex family of proteins or have mutiple regulatory mechanisms.

To this point, swelling-activated chloride conductances have mainly been studied using the whole-cell patch clamp configuration after induction of cell swelling by an applied transmembrane osmotic gradient. Cell swelling can be initiated during whole-cell recording either by increasing the osmolarity of the pipette solution or by lowering the osmolarity of the extracellular solution. In either case, the amount of cell swelling is difficult to control, because it depends not only on the osmotic gradient (as in intact cells), but also on the size of the pipette opening, on membrane permeability to water, and on mechanical properties of the cell membrane. These

variables have been modeled recently (Ross, Garber, and Cahalan, 1994). Because the cell interior under whole-cell recording is dialyzed by the infinite reservoir of solution in the patch pipette, the model predicts the ultimate disruption of the cell membrane due to uncontrolled swelling if a high enough osmotic gradient is applied. This prediction has been confirmed experimentally (Ross et al., 1994). Because of problems in controlling cell swelling during whole-cell recording, it is important to control for access resistance when comparing g_{Cl} obtained by patch clamp experiments on different cell lines. By monitoring SPQ fluorescence with video imaging, we developed a technique to assay g_{Cl} in intact cells under controlled conditions. The SPQ-quench experiments corroborated our patch clamp data on the time course and pharmacological sensitivity of g_{Cl}, and permitted a fairly accurate assessment of the threshold for channel activation by cell swelling.

Does P-Glycoprotein Form a Chloride Channel?

The model of P-glycoprotein as a swelling-activated Cl^- channel rests on the observation that transfection of P-glycoprotein cDNA into drug-sensitive cells resulted in the expression of swelling-activated Cl^- channels (Valverde et al., 1992). This observation was supported by experiments showing overlap in the pharmacological inhibition of drug transport.

g_{Cl} is not correlated with P-glycoprotein expression. During our patch clamp experiments, osmotic challenge with either hypoosmotic external solution or hyperosmotic internal solution resulted in cell swelling, which was invariably followed by the induction of g_{Cl} in both control or drug-resistant cell lines. We found that cell swelling induced g_{Cl} of similar magnitudes, rates of induction and biophysical properties, irrespective of P-glycoprotein expression or drug-transport activity (Figs. 3–5, Table I). After we observed large chloride conductances in the control NIH-3T3 fibroblasts, which were not reported by Valverde et al. (1992), we first ruled out the possibility of anomalous P-glycoprotein expression or drug-efflux activity in our cells. Direct assays of P-glycoprotein content and functional assays showed that our control cells do not express measurable amounts of P-glycoprotein. FACS analysis and confocal microscopy showed (Fig. 1) that P-glycoprotein was abundantly expressed in the drug-resistant cells (8226/Dox_{40} and NIH-3T3/MDR) but not in drug-sensitive cells (8226 myeloma and NIH-3T3 control). The transport function of P-glycoprotein in these cells was confirmed using R123-accumulation assays (Fig. 3). R123 accumulation was blocked by verapamil, a known inhibitor of P-glycoprotein-mediated transport. Thus, drug resistance was correlated with expression of P-glycoprotein in our cell lines. These results were confirmed and extended by measuring efflux rates for R123 (Figs. 12, 13, 15); rates were >60-fold faster in 8226/Dox_{40} than in 8226 myeloma cells, and >100-fold faster in 3T3/MDR cells compared with NIH-3T3 control cells. In control cells, verapamil had no effect on the rate of R123 loss, indicating undetectable functional expression of R123 (Fig. 12). Weaver and co-workers (1994, and personal communication) found more than 55,000 binding sites for the P-glycoprotein-specific monoclonal antibody, MRK-16, on NIH-3T3/MDR cells and fewer than 400 antibody binding sites on NIH-3T3 control cells (the limits of resolution of the measurement). In comparison, how many chloride channels are present? The

single-channel conductance has not been determined in these cells. If we take an estimate from noise analysis of 2 pS for similar, outwardly rectifying, swelling-activated Cl^- channels in lymphocytes (Cahalan and Lewis, 1994), the average number of channels per cell would be 14,000 and 16,000 channels per cell in drug-sensitive and -resistant NIH-3T3 cells, respectively. Thus, there appears to be no correspondence between the number of chloride channels and the number of P-glycoprotein molecules per cell. Regardless of the exact numbers, the near equality of g_{Cl} combined with the disparity in P-glycoprotein expression strongly argues that drug efflux and chloride channel functions are mediated by different proteins.

Activation of g_{Cl} consistently occurred with several combinations of pipette and bath solutions, whenever the cells were swollen and access resistance maintained. Most of our experiments were performed with solutions containing asymmetric Cl^- concentrations, providing a negative reversal potential to distinguish Cl^- currents from nonspecific leak currents; solutions containing symmetrical Cl^- were equally effective. Using NIH-3T3 cells obtained from the same source, and duplicating the solutions and voltage-clamp protocols used in previous studies (Gill et al., 1992; Valverde et al., 1992; Diaz, Valverde, Higgins, Rucareanu, and Sepulveda, 1993), we found equivalent g_{Cl} in both control and *MDR*-transfected cells. We also varied the stimulus for cell swelling by using Ringer solutions which were 90, 80, 70, or 67% hyposmotic. In all cases, g_{Cl} induction occurred to the same extent in both drug-sensitive and drug-resistant cell lines varying in P-glycoprotein expression by at least two orders of magnitude.

Our SPQ-quench measurements of swelling-activated g_{Cl} in intact cells suggest that P-glycoprotein expressing cells may be somewhat more sensitive to the effects of osmotic gradients than control cells (Fig. 10). We have shown previously (Ross et al., 1994) that the extent of cell swelling and g_{Cl} induction during whole-cell recording depends critically on several variables including pipette access resistance, as well as osmolyte concentration. We routinely monitored access resistance during whole-cell recording, and typically obtained values less than 5 MΩ. The use of large osmotic gradients (33% difference between intracellular and extracellular osmolarity) ensured maximal swelling and induction of g_{Cl}. In some patch clamp experiments, we observed spontaneous increases in access resistance, accompanied by artifactual decreases in g_{Cl} (data not shown). In general, g_{Cl} values reported previously on NIH-3T3/MDR cells were severalfold smaller than the currents we observed in control or transfected NIH-3T3 cells. The differences in experimental outcomes from previous work (Valverde et al., 1992) might be explained by the extent of cell swelling, the threshold for activation of g_{Cl}, the access resistance, or all three factors together. The opening of Cl^- channels may involve a cascade of events following cell swelling. P-glycoprotein expression may lead to pleiotropic changes that result in upregulation of a component in the pathway that links the cell's volume increase to channel activation. We have observed that control NIH-3T3 cells tend to be flatter than transfected NIH-3T3/MDR cells (data not shown), possibly making low access resistance more difficult to achieve, or reducing the degree of stretch in the surface membrane for a given increase in volume. An indirect role for P-glycoprotein might also explain a previous report that antisense inhibition in NIH-3T3/MDR cells

reduced g_{Cl} (Valverde et al., 1992). Recently, Altenberg et al., (1994*b*) reported finding volume-sensitive Cl^- channels in human breast cancer cells (BC19/3) after transfection with P-glycoprotein cDNA, but not in the parental cells (MCF-7). However, using our standard protocol, we found large outwardly rectifying Cl^- conductances in MCF-7 cells following cell swelling induced by hypotonic Ringer (data not shown). We also confirmed that the MCF-7 cells showed no evidence of P-glycoprotein expression, but have not pursued this comparison further (data not shown). g_{Cl} magnitudes reported by Altenberg and colleagues (1994*a*,*b*) in the drug-resistant BC19/3 cells were smaller than we observed in control MCF-7 cells, again suggesting suboptimal activation of g_{Cl}. We conclude that expression of P-glycoprotein does not alter g_{Cl}, with the caveat that the cells may have to be optimally swollen to reveal similar levels of g_{Cl}.

Drug efflux and g_{Cl} are pharmacologically separable. A second line of evidence used previously to link g_{Cl} to P-glycoprotein was the report that some agents block both drug efflux and g_{Cl} (Valverde et al., 1992; Diaz et al., 1993; Nilius et al., 1994). We have compared the ability of several agents to inhibit R123 transport and g_{Cl}. Valverde and colleagues (1992) reported that 100 μM verapamil blocked g_{Cl} and drug transport in NIH-3T3 cells transfected with P-glycoprotein; this was seen as evidence that P-glycoprotein forms both chloride channels and the drug transport pump. In 3T3/MDR cells, we determined a K_d of 0.39 μM for verapamil block of unidirectional R123 efflux, while 100 μM verapamil had little or no effect on g_{Cl} determined by whole-cell recording or by SPQ imaging in NIH-3T3/MDR cells (Figs. 6, 11, 12). We also found agents that blocked g_{Cl}, but not R123 efflux. For example, DIDS, tamoxifen, and NPPB blocked g_{Cl} at doses which did not block R123 efflux. Certain organic blockers of K^+, Na^+, and Ca^{2+}, but not Cl^-, channels have been shown to inhibit drug transport in mouse lymphoma cells, most likely not by virtue of channel block, but by interacting directly with P-glycoprotein (Weaver et al., 1993). Thus, there appears to be a clear dissociation between the pharmacology of g_{Cl} and the drug-efflux pump.

Not only was NPPB ineffective in blocking R123 efflux, but the rate of R123 efflux actually increased in the presence of NPPB. We propose that the enhanced efflux rate is due to greater access of the dye substrate to the P-glycoprotein efflux pump after collapse of the mitochondrial membrane potential. Using confocal microscopy, we determined that the cytoplasmic concentration of R123 increases after exposure to NPPB, an effect that is most likely related to its known protonophore activity (Lukacs et al., 1991), because the more effective protonophore CCCP further enhances the R123 efflux rate. CCCP also increases the cytoplasmic concentration of R123, but does not significantly affect R123 efflux in control NIH-3T3 cells. The results with mitochondrial uncouplers suggest that R123 efflux is limited by substrate access to P-glycoprotein in the surface membrane, and is rate limited by release from mitochondria. We checked the ability of verapamil to inhibit R123 efflux from NIH-3T3/MDR cells in the presence or absence of CCCP, and obtained K_d values of 0.26 μM and 0.39 μM, respectively (data not shown). The close agreement of these K_d values confirms that verapamil inhibits substrate efflux by affecting the pump rather than substrate availability.

Drug Efflux and g_{Cl} Are Not Mutually Exclusive

Gill et al. (1992) proposed a specific model in which a molecule of P-glycoprotein can function either as a pump or a channel, but not as both at the same time. According to this pump/channel model, substrate binding to P-glycoprotein drives the molecule into the pump conformation and channel activation is inhibited. In support, they reported: (*a*) during whole-cell recording, pipette addition of P-glycoprotein substrates inhibited the activation of g_{Cl}; (*b*) this inhibition could be reversed by substituting nonhydrolyzable analogues of ATP in the pipette solution; and (*c*) mutations in P-glycoprotein's nucleotide binding domain also made g_{Cl} insensitive to inhibition by substrates for the pump. Other investigators, using human colon adenocarcinoma cells (Rasola et al., 1994) and breast cancer cells (Altenberg et al., 1994*b*; Han, Altenberg, and Reuss, 1994), have had difficulty in reproducing these results. Han et al. (1994) found that of cytotoxic agents tested only vinblastine prevented the induction of g_{Cl} in BC19/3 cells, and suggested an indirect effect on the Cl^- channel. We have also been unable to replicate the inhibition of g_{Cl} by drug substrates of P-glycoprotein. Including doxorubicin or vincristine in the pipette solution did not affect g_{Cl} induction (Figs. 8, 9, Table II); dialysis of doxorubicin was confirmed by monitoring intracellular fluorescence. Thus, our results support the conclusion that g_{Cl} is not inhibited by substrate binding to P-glycoprotein.

A second prediction of the pump/channel model is that drug efflux should be inhibited if the molecule is driven to function as a Cl^- channel during cell swelling. Sardini, Mintenig, Valverde, Sepulveda, Gill, Hyde, Higgins, and McNaughton (1994) reported that cell swelling reduced the rate of doxorubicin efflux by 69% and 87.2% from NIH-3T3/MDR and S1/1.1 cells, respectively. However, in our experiments, cell swelling by 67% Ringer had no effect on R123 efflux (Fig. 15); the same stimulus activated g_{Cl} maximally in intact cells monitored with the SPQ-quench assay (Fig. 10). Similar results were reported by Altenberg et al., (1994*b*) in BC19/3 cells. In conclusion, our experiments are not consistent with the dual-function pump/channel hypothesis.

The authors gratefully acknowledge Dr. Lu Forrest for culturing and maintaining the cell lines used in this study and Ms. Sue DeMaggio for assistance with the FACS® analysis. Ms. Ruth Davis provided helpful suggestions on the manuscript. We thank Dr. Michael Gottesman and Dr. William Dalton for generously supplying the cell lines used in this study. We thank Dr. Jose Lutzky of the Department of Hematology-Oncology, UCI and Dr. John Fruehauf and Mr. Larry Eck of Oncotoech, Irvine, CA for helpful technical discussions.

Supported by NIH grants NS14609 and GM41514.

Original version received 28 June 1994 and accepted version received 7 September 1994.

REFERENCES

Ackerman, M. J., K. D. Wickman, and D. E. Clapham. 1994. Hypotonicity activates a native chloride current in *Xenopus* oocytes. *Journal of General Physiology.* 103:153–179.

Altenberg, G. A., J. W. Deitmer, D. C. Glass, and L. Reuss. 1994*a*. P-glycoprotein-associated Cl^- currents are activated by cell swelling but do not contribute to cell volume regulation. *Cancer Research.* 54:618–622.

Altenberg, G. A., C. G. Vanoye, E. S. Han, J. W. Deitmer, and L. Reuss. 1994*b*. Relationships between rhodamine 123 transport, cell volume, and ion-channel function of P-glycoprotein. *Journal of Biological Chemistry.* 269:7145–7149.

Arceci, R. J., F. Baas, R. Raponi, S. B. Horwitz, D. Housman, and J. M. Croop. 1990. Multidrug resistance gene expression is controlled by steroid hormones in the secretory epithelium of the uterus. *Molecular Reproduction and Development.* 25:101–109.

Arceci, R. J., K. Stieglitz, J. Bras, A. Schinkel, F. Baas, and J. Croop. 1993. Monoclonal antibody to an external epitope of the human *mdr1* P-glycoprotein. *Cancer Research.* 53:310–317.

Bruggemann, E. P., S. J. Currier, M. M. Gottesman, and I. Pastan. 1992. Characterization of the azidopine and vinblastine binding site of P-glycoprotein. *Journal of Biological Chemistry.* 267:21020–21026.

Cahalan, M. D., and R. S. Lewis. 1988. Role of potassium and chloride channels in volume regulation by T lymphocytes. *In* Cell Physiology of Blood. Society of General Physiologists Series. Vol. 43, R. B. Gunn and J. C. Parker, editors. Rockefeller University Press, New York. 281–301.

Cahalan, M. D., and R. S. Lewis. 1994. Regulation of chloride channels in lymphocytes. *In* Current Topics in Membranes and Transport. W. Guggino, editor. Academic Press, San Diego. 103–129.

Christensen, O., and E. K. Hoffmann. 1992. Cell swelling activates K^+ and Cl^- channels as well as nonselective, stretch-activated cation channels in Ehrlich ascites tumor cells. *Journal of Membrane Biology.* 129:13–36.

Dalton, W. S., T. M. Grogan, J. A. Rybski, R. J. Scheper, L. Richter, J. Kailey, H. J. Broxterman, H. M. Pinedo, and S. E. Salmon. 1989. Immunohistochemical detection and quantitation of P-glycoprotein in multiple drug-resistant human myeloma cells: association with level of drug resistance and drug accumulation. *Blood.* 73:747–752.

Diaz, M., M. A. Valverde, C. F. Higgins, C. Rucareanu, and F. V. Sepulveda. 1993. Volume-activated chloride channels in HeLa cells are blocked by verapamil and dideoxyforskolin. *Pflügers Archiv.* 422:347–353.

Doroshenko, P., and E. Neher. 1992. Volume-sensitive chloride conductance in bovine chromaffin cell membrane. *Journal of Physiology.* 449:197–218.

Ehring, G. R., Y. V. Osipchuk, and M. D. Cahalan. 1994. Volume-activated chloride channels in drug-sensitive and -resistant cell lines. *Biophysical Journal.* 66:A142. (Abstr.)

Estacion, M. 1991. Characterization of ion channels seen in subconfluent human dermal fibroblasts. *Journal of Physiology.* 436:579–601.

Falke, L. C., and S. Misler. 1989. Activity of ion channels during volume regulation by clonal N1E115 neuroblastoma cells. *Proceedings of the National Academy of Sciences, USA.* 86:3919–3923.

Frizzell, R. A., and W. H. Cliff. 1992. No common motif. *Current Biology.* 2:285–287.

Georges, E., G. Bradley, J. Gariepy, and V. Ling. 1990. Detection of P-glycoprotein isoforms by gene-specific monoclonal antibodies. *Proceedings of the National Academy of Sciences, USA.* 87:152–156.

Gill, D. R., S. C. Hyde, C. F. Higgins, M. A. Valverde, G. M. Mintenig, and F. V. Sepulveda. 1992. Separation of drug transport and chloride channel functions of the human multidrug resistance P-glycoprotein. *Cell.* 71:23–32.

Gottesman, M. M., and I. Pastan. 1993. Biochemistry of multidrug resistance mediated by the mutidrug transporter. *Annual Review of Biochemistry.* 62:385–427.

Han, E. S., G. A. Altenberg, and L. Reuss. 1994. Substrate transport does not prevent P-glycoprotein-associated Cl^- currents activated by cell swelling. *Biophysical Journal.* 66:A99 (Abstr.)

Higgins, C. F. 1992. ABC transporters: from microorganisms to man. *Annual Review of Cell Biology.* 8:67–113.

Hitchins, R. N., D. H. Harman, R. A. Davey, and D. R. Bell. 1988. Identification of a multidrug resistance associated antigen (P-glycoprotein) in normal human tissues. *European Journal of Cancer and Clinical Oncology.* 24:449–454.

Hoffmann, E. K., and L. O. Simonsen. 1989. Membrane mechanisms in volume and pH regulation in vertebrate cells. *Physiological Reviews.* 69:315–382.

Illsley, N. P., and A. S. Verkman. 1987. Membrane chloride transport measured using a chloride-sensitive fluorescent probe. *Biochemistry.* 26:1215–1219.

Kelly, M. E. M., S. J. Dixon, and S. M. Sims. 1994. Outwardly rectifying chloride current in rabbit osteoclasts is activated by hypoosmotic stimulation. *Journal of Physiology.* 475:377–389.

Kessel, D., W. T. Beck, D. Kukuruga, and V. Schulz. 1991. Characterization of multidrug resistance by fluorescent dyes. *Cancer Research.* 51:4665–4670.

Kioka, N., J. Tsubota, Y. Kakehi, T. Komano, M. M. Gottesman, I. Pastan, and K. Ueda. 1989. P-glycoprotein gene (*MDR1*) cDNA from human adrenal: normal P-glycoprotein carries Gly185 with an altered pattern of multidrug resistance. *Biochemical and Biophysical Research Communications.* 162:224–231.

Kubo, M., and Y. Okada. 1992. Volume-regulatory Cl^- channel currents in cultured human epithelial cells. *Journal of Physiology.* 456:351–371.

Lampidis, T. J., J. N. Munck, A. Krishan, and H. Tapiero. 1985. Reversal of resistance to rhodamine 123 in adriamycin-resistant Friend leukemia cells. *Cancer Research.* 45:2626–2631.

Lampidis, T. J., C. Castello, A. del Giglio, B. C. Pressman, P. Viallet, K. W. Trevorrow, G. K. Valet, H. Tapiero, and N. Savaraj. 1989. Relevance of the chemical charge of rhodamine dyes to multiple drug resistance. *Biochemical Pharmacology.* 38:4267–4271.

Lewis, R. S., P. E. Ross, and M. D. Cahalan. 1993. Chloride channels activated by osmotic stress in T lymphocytes. *Journal of General Physiology.* 101:801–826.

Lindau, M., and E. Neher. 1988. Patch-clamp techniques for time-resolved capacitance measurements in single cells. *Pflügers Archiv.* 411:137–146.

Ludescher, C., J. Thaler, D. Drach, J. Drach, M. Spitaler, C. Gattringer, H. Huber, and J. Hofmann. 1992. Detection of activity of P-glycoprotein in human tumour samples using rhodamine 123. *British Journal of Haematology.* 82:161–168.

Lukacs, G. L., A. Nanda, O. D. Rotstein, and S. Grinstein. 1991. The chloride channel blocker 5-nitro-2-(3-phenylpropyl-amino) benzoic acid (NPPB) uncouples mitochondria and increases the proton permeability of the plasma membrane in phagocytic cells. *FEBS Letters.* 288:17–20.

McEwan, G. T., J. Hunter, B. H. Hirst, and N. L. Simmons. 1992. Volume-activated Cl^- secretion and transepithelial vinblastine secretion mediated by P-glycoprotein are not correlated in cultured human T_{84} intestinal epithelial layers. *FEBS Letters.* 304:233–236.

Neher, E. 1992. Correction for liquid junction potentials in patch clamp experiments. *Methods in Enzymology.* 207:123–131.

Neyfakh, A. A. 1988. Use of fluorescent dyes as molecular probes for the study of multidrug resistance. *Experimental Cell Research.* 174:168–176.

Nilius, B., M. Oike, I. Zahradnik, and G. Droogmans. 1994. Activation of a Cl^- current by hypotonic volume increase in human endothelial cells. *Journal of General Physiology.* 103:787–805.

Osipchuk, Y. V., G. R. Ehring, and M. D. Cahalan. 1994. Pharmacological sensitivities of volume-activated chloride conductance and rhodamine 123 efflux in drug-sensitive and -resistant cell lines. *Biophysical Journal.* 66:A142. (Abstr.)

Pollard, C. E. 1993. A volume-sensitive Cl^- conductance in a mouse neuroblastoma x rat dorsal root ganglion cell line (F11). *Brain Research.* 614:178–184.

Rasola, A., L. J. Galietta, D. C. Gruenert, and G. Romeo. 1992. Ionic selectivity of volume-sensitive currents in human epithelial cells. *Biochimica et Biophysica Acta.* 1139:319–323.

Rasola, A., L. J. Galietta, D. C. Gruenert, and G. Romeo. 1994. Volume-sensitive chloride currents in four epithelial cell lines are not directly correlated to the expression of the *MDR-1* gene. *Journal of Biological Chemistry.* 269:1432–1436.

Ross, P. E., S. S. Garber, and M. D. Cahalan. 1994. Membrane chloride conductance and capacitance in Jurkat T lymphocytes during osmotic swelling. *Biophysical Journal.* 66:169–178.

Sardini, A., G. M. Mintenig, M. A. Valverde, F. V. Sepulveda, D. R. Gill, S. C. Hyde, C. F. Higgins, and P. A. McNaughton. 1994. Cell swelling inhibits drug efflux from cells expressing the multidrug resistance phenotype. *Journal of Physiology.* 475:95P. (Abstr.)

Solc, C. K., and J. J. Wine. 1991. Swelling-induced and depolarization-induced Cl-channels in normal and cystic fibrosis epithelial cells. *American Journal of Physiology.* 261:C658–C674.

Stoddard, J. S., J. H. Steinbach, and L. Simchowitz. 1993. Whole cell Cl^- currents in human neutrophils induced by cell swelling. *American Journal of Physiology.* 265:C156–C165.

Tanaka, S., S. J. Currier, E. P. Bruggemann, K. Ueda, U. A. Germann, I. Pastan, and M. M. Gottesman. 1990. Use of recombinant P-glycoprotein fragments to produce antibodies to the multidrug transporter. *Biochemical and Biophysical Research Communications.* 166:180–186.

Toth, K., M. M. Vaughan, H. K. Slocum, M. A. Arredondo, H. Takita, R. M. Baker, and Y. M. Rustum. 1994. New immunohistochemical "sandwich" staining method for *mdr1* P-glycoprotein detection with JSB-1 monoclonal antibody in formalin-fixed, paraffin-embedded human tissues. *The American Journal of Pathology.* 144:227–236.

Tseng, G. N. 1992. Cell swelling increases membrane conductance of canine cardiac cells: evidence for a volume-sensitive Cl channel. *American Journal of Physiology.* 262:C1056–C1068.

Tsuruo, T., H. Iida, S. Tsukagoshi, and Y. Sakurai. 1981. Overcoming of vincristine resistance in P388 leukemia in vivo and in vitro through enhanced cytotoxicity of vincristine and vinblastine by verapamil. *Cancer Research.* 41:1967–1972.

Tsuruo, T., H. Iida, K. Naganuma, S. Tsukagoshi, and Y. Sakurai. 1983. Promotion by verapamil of vincristine responsiveness in tumor cell lines inherently resistant to the drug. *Cancer Research.* 43:808–813.

Ueda, K., C. Cardarelli, M. M. Gottesman, and I. Pastan. 1987. Expression of a full-length cDNA for the human "*MDR1*" gene confers resistance to colchicine, doxorubicin, and vinblastine. *Proceedings of the National Academy of Sciences, USA.* 84:3004–3008.

Valverde, M. A., M. Diaz, F. V. Sepulveda, D. R. Gill, S. C. Hyde, and C. F. Higgins. 1992. Volume-regulated chloride channels associated with the human multidrug-resistance P-glycoprotein. *Nature.* 355:830–833.

van Kalken, C., G. Giaccone, P. van der Valk, C. M. Kuiper, M. M. Hadisaputro, S. A. Bosma, R. J. Scheper, C. J. Meijer, and H. M. Pinedo. 1992. Multidrug resistance gene (P-glycoprotein) expression in the human fetus. *The American Journal of Pathology.* 141:1063–1072.

van Kalken, C. K., P. van der Valk, M. M. Hadisaputro, R. Pieters, H. J. Broxterman, C. M. Kuiper, G. L. Scheffer, A. J. Veerman, C. J. Meyer, and R. J. Scheper. 1991. Differentiation dependent expression of P-glycoprotein in the normal and neoplastic human kidney. *Annals of Oncology.* 2:55–62.

Weaver, J. L., P. S. Pine, A. Aszalos, P. V. Schoenlein, S. J. Currier, R. Padmanabhan, and M. M. Gottesman. 1991. Laser scanning and confocal microscopy of daunorubicin, doxorubicin, and rhodamine 123 in multidrug-resistant cells. *Experimental Cell Research.* 196:323–329.

Weaver, J. L., G. J. Szabo, P. S. Pine, M. M. Gottesman, S. Goldenberg, and A. Aszalos. 1993. The effect of ion channel blockers, immunosuppressive agents, and other drugs on the activity of the multi-drug transporter. *International Journal of Cancer.* 54:456–461.

Weaver, J. L., L. C. McKinney, P. V. Schoenlein, S. Goldenberg, M. M. Gottesman, and A. Aszalos. 1994. Volume regulation and MDRl protein function in MDRl-transfected and parental cell lines. *Biophysical Journal.* 66:A217. (Abstr.)

Welsh, M. J., M. P. Anderson, D. P. Rich, H. A. Berger, G. M. Denning, L. S. Ostedgaard, D. N. Sheppard, S. H. Cheng, R. J. Gregory, and A. E. Smith. 1992. Cystic fibrosis transmembrane conductance regulator: a chloride channel with novel regulation. *Neuron.* 8:821–829.

Worrell, R. T., A. G. Butt, W. H. Cliff, and R. A. Frizzell. 1989. A volume-sensitive chloride conductance in human colonic cell line T_{84}. *American Journal of Physiology.* 256:C1111–C1119.

Zhang, J., R. L. Rasmusson, S. K. Hall, and M. Lieberman. 1993. A chloride current associated with swelling of cultured chick heart cells. *Journal of Physiology.* 472:801–820.